

ASD-TR-61-467

PART II

88072

**INTERFACE DAMPING AT RIVETED JOINTS,
PART II: DAMPING AND FATIGUE MEASUREMENTS**

✓
D. C. G. EATON
D. J. MEAD

UNIVERSITY OF SOUTHAMPTON

AF61(052)-504

TECHNICAL REPORT ASD-TR-61-467, PART II

PROPERTY OF

LTV VOUGHT AERONAUTICS DIVISION

LIBRARY

DEC 06 1965

AUGUST 1965
✓

=USAF Aeronautical Systems Div.

AIR FORCE MATERIALS LABORATORY
RESEARCH AND TECHNOLOGY DIVISION
AIR FORCE SYSTEMS COMMAND
WRIGHT-PATTERSON AIR FORCE BASE, OHIO

INTERFACE DAMPING AT RIVETED JOINTS
PART II: DAMPING AND FATIGUE MEASUREMENTS

D. C. G. EATON
D. J. MEAD

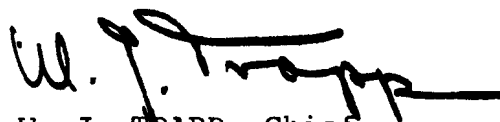
FOREWORD

This report was prepared by the University of Southampton, Department of Aeronautics and Astronautics, Southampton, U. K. under USAF Contract No. AF-61(052)-504. The contract was initiated under Project No. 7351, "Metallic Materials", Task No. 735106, "Behavior of Metals". The contract was administered by the European Office, Office of Aerospace Research. The work was monitored by the AF Materials Laboratory, Research and Technology Division, Air Force Systems Command, Wright-Patterson Air Force Base, under the direction of Mr. W. J. Trapp.

This report covers work from 31 April 1960 to 31 April 1961.

The manuscript was released by the authors June 1963, for publication as an RTD technical report.

This technical report has been reviewed and is approved.



W. J. TRAPP, Chief
Strength and Dynamics Branch
Metals and Ceramics Division
Air Force Materials Laboratory

ABSTRACT

This report describes experiments carried out to verify the theories of ASD Technical Report 61-467, Part I, which predicted the energy dissipation in a simple lap joint with a visco-elastic interfacial layer. The effect of the visco-elastic layer on the fatigue life of such a joint is also investigated.

The complex shear modulus of the visco-elastic material used (Polyvinyl Acetate) has been measured for a range of frequencies and temperatures. This permitted an optimum joint configuration to be chosen and provided data for comparing theoretical with experimental values of the energy dissipated in the joint.

Experiments on singly riveted lap joints have indicated that a considerable damping increment can be obtained by the addition of the damping layer, although the magnitude varies considerably with frequency and temperature.

Fatigue tests on singly riveted lap joints have indicated that, within the limits of the investigation, the presence of the visco-elastic layer improves the fatigue life of the joint.

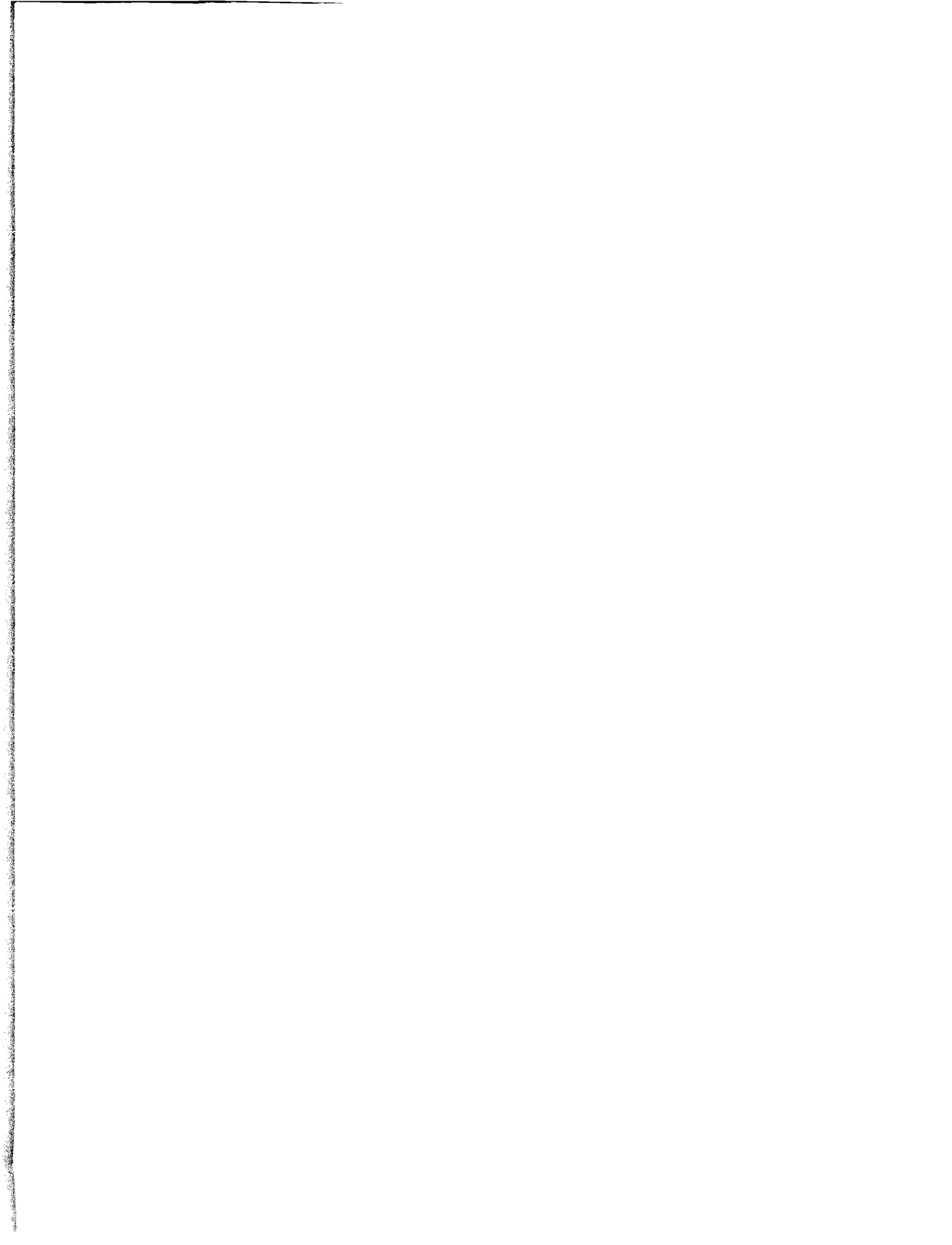


TABLE OF CONTENTS

Page No.

1.	Introduction	1
2.	The Measurement of the Complex Shear Modulus of a Visco-Elastic Material (Polyvinyl Acetate)	2
2.1	The Measuring Technique	2
2.1.1	Theoretical Background	2
2.2	The Test Rig	4
2.3	The Experimental Technique	4
2.4	Discussion of Results	5
3.	Stiffness and Damping Measurements on a Single Riveted Lap Joint	5
3.1	The Test Requirements	5
3.2	Analysis by means of the Energy Input Technique	6
3.3	The Test Rig	7
3.4	Experimental Investigations	9
3.4.1	Calibration of the Measuring Equipment and the System	9
3.5	Discussion of Results	11
4.	Fatigue Test on Simple Riveted Lap Joints with and without a Damping Layer	12
4.1	Introduction	12
4.2	The Fatigue Test Apparatus	13
4.2.1	The Fatigue Test Rig	13
4.2.2	Maintaining a Constant Test Load on the Joint... ..	14
4.2.3	Miscellaneous Additional Facilities	15
4.2.4	Preparation of the Specimens	16
4.3	Calibration of the Rig	16
4.4	Test Procedure and Observations	17
4.5	Discussion of Results	19
5.	Conclusions	21
	Appendix I A Summary of the Rigid Plate Theory	24
	Appendix II Theoretical Estimation of the Plate Load at the Rivet in a Joint with a Visco-Elastic Layer	25
	References	27

ILLUSTRATIONS

Figure		Page
1	Measurement of the Complex Shear Modulus: The Configuration and the Dynamic Equilibrium of Forces.	28
2	Apparatus for Measuring the Complex Shear Modulus of Visco-Elastic Materials - General View	29
3	Apparatus for Measuring the Complex Shear Modulus of Visco-Elastic Materials - Exploded View	30
4	Block Diagram of the Exciting and Measuring Systems. Complex Shear Modulus Apparatus	31
5	Variation with Frequency and Temperature of the Real Part of the Complex Shear Modulus	32
6	Variation with Frequency and Temperature of the Material Loss Factor.	33
7a	Details of Joints for Damping Measurements	34
7b	Diagram of the Bar with Joint.	34
8	Apparatus for Measuring the Stiffness and Damping of a Riveted Joint with a Damping Layer - General View	35
9	Apparatus for Measuring the Stiffness and Damping of a Riveted Joint with a Damping Layer - Central Portion	36
10	Block Diagram of the Apparatus for Measuring the Stiffness and Damping Properties of a Riveted Joint	37
11	The Variation with Load Amplitude of the Energy Dissipated Per Cycle at a Conventional Riveted Joint	38
12	The Variation with Frequency of the Energy Dissipated Per Cycle at a Joint with a Visco-Elastic Interface. Joint Temperature = 21°C.	39
13	The Variation with Frequency of the Energy Dissipated Per Cycle at a Joint with a Visco-Elastic Interface. Joint Temperature = 24.5°C	40
14	The Variation with Frequency of the Energy Dissipated Per Cycle at a Joint with a Visco-Elastic Interface. Joint Temperature = 30°C.	41
15	Fatigue - Rig for Testing Riveted Joints	42
16	Line Diagram of the Self Excited Method Applied to the Fatigue Rig.	43
17	Details of the Fatigue Test Specimens	44
18	Fatigue Curves for a Singly-Riveted Conventional Lap Joint Subjected to Simple Harmonic Loading.	45
19	Fatigue Curves for a Singly-Riveted Lap Joint with a Visco-Elastic Interface Subjected to Simply Harmonic Loading. Joint Temperature = 30°C	46

SYMBOLS

b	plate width
d	thickness of the visco-elastic interfacial layer
f	non-dimensional energy dissipation function
g	normalised imaginary part of the joint stiffness (see § 3 equation 3.1)
h	plate thickness
i	$\sqrt{-1}$
k_i	the real part of the complex shear stiffness of the interfacial layer
k_r	rivet stiffness
k_o	joint stiffness (see § 3.2)
k^*	complex shear stiffness
ℓ	plate overlap length
t	time
$u_o(t)$	relative displacement of two inextensible plates
$u_1(t), u_2(t)$	longitudinal displacements of two sections of a bar
$u_j(t)$	relative displacement across a joint
E	modulus of elasticity of plate material
G	real part of complex shear modulus
$G^* = G(1 + i\beta)$	complex shear modulus
P(t)	load applied to a system
P_i	load passing through visco-elastic layer

p_0	amplitude of harmonic load
p_p	load in plate at rivet
β	loss factor, i.e. normalised imaginary part of complex shear modulus of the damping layer
ϵ	phase lead of displacement relative to exciting force
μ	mass per unit length
ϕ	shear parameter
γ	joint loss factor
ω	circular frequency
Δ	energy dissipated per load cycle (elastic plates)
Δ_s	energy dissipated per load cycle (rigid plates)

1. Introduction

In Part I⁽¹⁾ a theoretical examination was made of the structural damping increments that could be obtained by the insertion of a visco-elastic layer between the plates of riveted joints. Consideration was given to a lap joint having anti-symmetry about its single rivet, and being subjected to a simple-harmonic longitudinal loading.

The contents of Part II are concerned with experiments carried out to assess how well the theories of Part I describe the energy dissipation in a simple lap joint. In addition the effect of the visco-elastic layer on the fatigue life of such a joint has been examined.

It was first necessary to measure the dynamic shear properties of the visco-elastic material which was to be used for the layer (a poly-vinyl acetate resin). The complex shear modulus of the material was measured over a range of temperatures and frequencies (see § 2). These data provided essential information both in assessing the suitability of the material and in correlating theoretical and experimental assessments of the energy dissipated at the joint.

Tests were next carried out to determine the energy dissipation in a simple singly riveted lap joint (see § 3). An attempt was made to ensure that a maximum dissipation of energy would occur for one particular excitation frequency and temperature combination used in the experiment.

Having measured the rivet stiffness and the complex shear modulus of the visco-elastic material, it was possible to select the interface thickness for maximum energy dissipation using the 'rigid plate theory' described in Part I. In measuring the variation of the energy dissipated at the joint with temperature and frequency, care was taken to ensure that the loading conditions imposed on the joint were as close as possible to those assumed in the theoretical analysis. Using the measured complex shear modulus of the interface material, it was possible to compare the experimental results with those of the theoretical work.

The final experimental investigation was concerned with the fatigue life of such joints, (see § 4). Obviously, if the insertion of a visco-elastic layer seriously impairs the fatigue life of the joint, the exercise would defeat its own object, namely, of increasing the fatigue life of the aircraft

structure. Inserting the material, whilst eliminating fretting between the plates, also eliminates frictional adhesion and thus reduces the joint stiffness. The material must therefore counteract this by having a good load transmitting capacity, without being subject to early fatigue failure.

Due to the inherent complexity of the fatigue problem it was not possible to carry out a comprehensive programme in the time available. The investigation was therefore limited to testing the singly riveted lap joint specimens under harmonic longitudinal loading at constant load amplitude. Two batches of specimens were tested, with and without damping layers. These tests were carried out at a number of load levels to obtain some characteristic 'S-N' curves. The investigation produced a qualitative picture of salient fatigue characteristics.

It has been possible to draw some general conclusions concerning the feasibility of this damping technique and these are outlined in § 5.

2. The Measurement of the Complex Shear Modulus of a Visco-Elastic Material (Polyvinyl Acetate)

2.1 The Measuring Technique

2.1.1 Theoretical Background

A dynamic (sinusoidal) technique was used to measure the complex shear modulus of the damping material. In this system the material was subjected to dynamic shearing stresses by a simple harmonic exciting force. The magnitude of this force and the velocity of deformation were detected by electro-mechanical transducers (a strain gauge force transducer and an electro-magnetic velocity transducer). The method of applying these dynamic shearing stresses is indicated by the line diagram of Figure 1a.

The equation of motion of this system, using the co-ordinate system of Figure 1a, is:

$$\vec{P} \cos \omega t - k^* \vec{u}(t) = M\ddot{u}(t), \quad \dots (2.1)$$

where $\vec{u}(t)$ is the shear deflection of the material (and thus of the driving arm shown in the figure),

$$\text{and } \vec{u}(t) = \vec{u}_0 \cos (\omega t + \gamma).$$

k^* is the complex shear stiffness of the material and may be written in the form $k^* = k + ih$.

Using the notation for the complex shear modulus:

$$G^* = G(1 + i\beta), \text{ then:}$$

$$k = \frac{Gb\ell}{d} \quad \text{and} \quad h = \frac{Gb\ell\beta}{d} \quad (\text{see Figure 1a}). \quad \dots (2.2)$$

It is convenient to represent equation 2.1 in terms of a vector diagram of forces as shown in Figure 1b. \vec{P} represents the harmonic exciting force which can be considered to rotate clockwise with an angular velocity corresponding to the frequency of excitation. The diagram therefore represents the equilibrium of the force, \vec{P} , with the elastic restoring force of the material, $k\vec{u}_0$, the damping force $ih\vec{u}_0$ and the inertia force, $M\omega^2\vec{u}_0$. The magnitudes of the actual forces at any instant can be considered to be represented by the projection of these vectors on OY.

It is readily seen from this diagram that

$$k = \frac{|\vec{P}|}{|\vec{u}_0|} \cos\eta + M\omega^2$$

$$\text{and} \quad h = \frac{|\vec{P}|}{|\vec{u}_0|} \sin\eta$$

i.e. using equation (2.2)

$$G = \left(\frac{|\vec{P}|}{|\vec{u}_0|} \cdot \cos\eta + M\omega^2 \right) d/bl$$

$$\text{and} \quad \beta G = \frac{|\vec{P}|}{|\vec{u}_0|} (\sin\eta) d/bl.$$

$|\vec{P}|$ and $|\vec{u}_0|$ may be measured with the aid of the force and velocity transducers, respectively. The phase relationship, η , is determined from the phase relationship between the electrical signals from the transducers which may be measured with a phase-meter (see § 2.3). The complex shear modulus can therefore be readily established for a particular excitation frequency and material temperature.

2.2 The Test Rig

A photograph of the test rig equipment is shown in Figure 2. Two wafers of the visco-elastic material, square in cross section, and of uniform thickness, were affixed to corresponding identical areas on two platens and a central arm. The resulting configuration was that of a 'double lap joint' as is shown in Figure 3. These platens were firmly bolted to a rigid vertical pillar which was mounted on a rigid 'Paxolin' block for temperature insulation. This block was bolted down on to a mild steel base which was in turn bolted to the steel runners of a heavy foundation block.

A simple harmonic load was applied to the central arm by an electro-magnetic vibration exciter, which was also bolted to the runners of the foundation block. This applied load was measured with a strain gauge force transducer which formed an integral part of the central arm (see Figures 2 and 3). Thus simple harmonic shearing stresses were applied to the wafers. The corresponding deformations were detected using an electro-magnetic velocity transducer (Figure 3). The phase measurement was made using a Solartron resolved components indicator.

Facilities were incorporated to regulate the material temperature. The heat exchange process was carried on by a fluid circulating round a closed circuit which 'enveloped' the test specimens and the immediate test rig components (see Figure 2). The device was thermostatically controlled and the material temperature was estimated from thermocouples placed in close proximity to the wafers.

2.3 The Experimental Technique

In determining the variation of the complex shear modulus the tests were conducted at a low shear strain amplitude (0.3%). In this region initial tests indicated that the material behaved linearly, so that non-linear problems were avoided.

The electrical equipment used for loading the material and measuring the response is shown in Figure 4. The measuring procedure was carried out at constant temperature for a range of frequencies (100 c/s to 1,000 c/s in 50 c/s increments) and this was repeated for a range of temperatures (12°C to 30°C in 2°C increments).

2.4 Discussion of the Results

Curves have been obtained for the variation with excitation frequency and temperature of the real part of the complex shear modulus G and the corresponding material loss factor, β , (Figures 5 and 6).

The curves of G exhibit characteristics common to many visco-elastic materials. In the frequency range covered, G decreases with increasing temperature but increases with increasing frequency. It can thus be readily seen that an increase in frequency is qualitatively equivalent to a decrease in temperature in its effect on the real part of the complex shear modulus. Ferry and others^(2,3) have used this fact to extend their experimental results to cover a wide range of temperature and frequency. The technique used is known as 'The Method of Reduced Variables'.⁽⁴⁾ G should have limiting values at high and low frequencies. There is some evidence of this at the high frequency end of the range (approaching 1,000 c/s) but the frequency range did not extend to sufficiently low values to disclose a lower limit for G .

The curves for the variation in loss factor with frequency do not behave in a simple fashion. Whilst there are no sudden discontinuities with changes in frequency at any temperature level, there are considerable fluctuations with temperature increase, more markedly at the highest temperatures considered. No curve smoothing has been applied to these results. This is often performed when applying the Method of Reduced Variables. Rapid changes in the loss factor have been observed by other experimenters. However, inaccuracies in the measuring technique may have affected the results.

3. Stiffness and Damping Measurements on a Single Riveted Lap Joint

3.1 The Test Requirements

In assessing the usefulness of the theoretical analysis, and in particular in complying with the physical restrictions imposed by the boundary conditions of the theoretical work, it was desirable to satisfy the following requirements:

- (i) The joint should not be subjected to bending stresses.
- (ii) The joint should be subjected to a longitudinal simple harmonic exciting force.

- (iii) It should be possible to vary the temperature and excitation frequency (within the limits of the complex shear modulus data) so that a corresponding variation in the theoretical parameters could be investigated.
- (iv) It should be possible to measure the stiffness of the rivet with the same equipment.
- (v) The magnitude of the exciting force should be sufficient to facilitate accurate measurements of the energy dissipation.

These requirements were met by using the following technique. The joint was inserted at the centre of a bar which had masses on its ends and which was made to vibrate in its fundamental longitudinal 'free-free' mode. The joint was therefore at a displacement node. The bar was excited by an axial force at one end, so that the joint was subjected to the inertia forces set up in the bar. Due to the 'dynamic magnification factor' of the system, sufficiently high dynamic loads were applied to the joint. By suitable alignment of the joint configuration (see Figure 7a) it was possible to ensure that a purely axial force was applied to the joint without any appreciable bending stresses being developed. A suitable choice of bar dimensions and end masses enabled a frequency range of about 200 c/s to 800 c/s to be covered. It was also possible to measure the rivet stiffness with the devised system. The temperature of the joint could be varied without serious difficulty.

The use of this resonance device readily lent itself to a particular application of the energy input measuring technique (5).

3.2 Analysis by means of the Energy Input Technique

Consider the vibrating system shown in Figure 7b, which represents the long bar with end masses. The joint at the centre separates the bar into the sections 1 and 2. If the exciting force is applied at the left hand end, the total load exerted on the joint is equal to the sum total of the inertia forces on section 2 (assuming that no external damping forces act on section 2). Denote the local, longitudinal acceleration in section 2 by \ddot{u}_2 and the local mass per unit length by μ . The total force on the joint is therefore

$$P(t) = - \int_{l/2}^l \ddot{u}_2 \mu dx.$$

Let the displacement of one end of the joint relative to the other be $u_j(t)$. If the total complex longitudinal stiffness of the joint is $k_0(1 + ig)$, then we must have

$$k_0(1 + ig) u_j(t) = P(t) = - \int_{l/2}^l \ddot{u}_2 \mu \, dx \quad \dots (3.1)$$

Now the overall damping of the actual system tested was small enough to justify the assumption that at the fundamental resonant frequency, the longitudinal harmonic accelerations at all points in section 2 were in phase with one another.

We therefore put $u_2 = \bar{u}_2(x) \sin \omega t$

$$\text{so that } \ddot{u}_2 = - \omega^2 \bar{u}_2(x) \sin \omega t. \quad \dots (3.2)$$

$$\text{Also, } u_j(t) = \bar{u}_j \sin(\omega t + \epsilon). \quad \dots (3.3)$$

$$\text{Hence } P(t) = \omega^2 \int_{l/2}^l \bar{u}_2(x) \mu \, dx \cdot \sin \omega t = \bar{P} \sin \omega t \quad \dots (3.4)$$

$\bar{u}_2(x)$, \bar{u}_j and \bar{P} are the amplitudes of the harmonically varying parameters.

It is now readily shown that the energy dissipated in the joint per cycle is given by

$$\Delta = \pi \bar{P} \bar{u}_j \sin \epsilon = \pi \left\{ \omega^2 \int_{l/2}^l \bar{u}_2(x) \mu \, dx \right\} \bar{u}_j \sin \epsilon.$$

Δ may therefore be determined by measuring the displacement function $\bar{u}_2(x)$, the relative displacement amplitude across the joint, \bar{u}_j , and the phase difference between the displacements $u_j(t)$ and u_2 .

3.3 The Test Rig

Figure 8 shows a photograph of the rig. An aluminium alloy bar was manufactured in two halves which were joined together by a central portion that contained the specimen joint. The overall length of the composite bar was approximately six

feet. The inner ends of the two halves were threaded for the attachment of the central portion, as were the extremities for the attachment of cylindrical end masses. End masses of different sizes were used to alter the resonant frequency of the system. In this way a frequency range of about 200 to 800 c/s could be covered.

Five calibrated barium-titanate accelerometers were used to measure local accelerations at intervals along the lower half of the bar in order to measure the longitudinal accelerations and the corresponding inertia forces.

Figure 9 shows the assembly of the central portion. This consisted of two short cylindrical bars each having a milled-out tongue to represent a lap joint plate. In order to provide axial loading and minimum bending of the plates, the tongues were each offset from the centre line of the bar by an amount equal to half the thickness of the interface as shown in Figure 7a. The relative velocity across the ends of the joint was measured with the aid of the electro-magnetic velocity transducer forming an integral part of the central portion.

The resulting composite bar was hung from a flexible aluminium support attached to a rigid steel frame as shown in Figure 8. The aluminium 'portal' was designed to have a fundamental flexural frequency considerably lower than those in the frequency range covered.

A small electro-magnetic exciter driven by the usual oscillator-power amplifier arrangement was used to excite the bar. The exciter was bolted to the steel frame.

A second velocity transducer was used to measure the phase angle between the joint velocity and lower bar velocity. The coil was attached to the lower end of the bar and its magnet mounted separately. Care was taken in the design and construction of the rig over items such as threaded couplings, clearance of moving parts, etc., to keep any extraneous damping to a minimum.

Details of the layout of the exciting and measuring equipment are given in a block diagram (Figure 10).

Facilities were provided to raise the joint temperature and to obtain an accurate estimate of this temperature.

3.4 Experimental Investigations

3.4.1 Calibration of the Measuring Equipment and the System

The accelerometers and velocity transducers were calibrated using established techniques.

The mass distribution was considered apportioned to the accelerometer locations. Knowing the acceleration at these points it was possible to estimate the inertia forces applied to the joint. In order to check the accuracy of these measurements a statically calibrated strain gauge force transducer was inserted at the bar centre. This device replaced the central portion and was of similar dimensions. It was found that the force measured by this means corresponded closely to the estimated inertia force, the greatest variance being about 7% at the highest frequency.

With the aid of the central force transducer it was possible to obtain some idea of the bending strains set up in the joint plates. The bending strain in the force transducer plate was about 1% of the corresponding direct strain.

It was also possible to make an additional check on the accuracy likely to be obtained from the transducer measuring the relative velocity across the joint. Readings were taken of the force transducer and corresponding velocity transducer signals. Knowing the geometry of the central portion, its elastic modulus and the magnitude of the applied force, it was possible to estimate the stretching of the central portion which could then be compared with that calculated from the corresponding signal from the velocity transducer. An agreement to within 8% at the worst was obtained, again at the highest frequency.

Finally, checks were made to see that no modes other than the longitudinal modes were set up on exciting the system, with the joint in position. The phase relationships between accelerometers was observed. A rigorous investigation was conducted with accelerometers at the best positions for observing other conceivable modes. There was no evidence of any other modes being excited at the longitudinal resonant frequencies.

3.4.2 Determination of the Stiffness and Damping of the Riveted Joints

An experiment was conducted to estimate the stiffness of the type of formed rivet that would be used in the joint with a visco-elastic layer. Because of the presence of the layer the rivet shank length would be increased by an amount equal to the

thickness of the layer. This, together with the removal of the friction between the plates would result in a reduction in effective rivet stiffness. In order to measure this rivet stiffness a central portion was riveted together with a gap between the joint plates equal to the thickness of the layer. The bar was excited and measurements made of the inertia forces applied to the joint and the corresponding velocity transducer reading. After corrections had been made to the latter value to allow for the stretching of the joint plates and bars of the central portion, it was possible to estimate the rivet deflection. It was possible therefore to obtain the rivet stiffness. The experiment was repeated for different frequencies and a mean value of 6.9×10^4 lb/inch was taken for the rivet stiffness. [Note: (Rivet stiffness)⁻¹ is the difference between the flexibility of the jointed specimen and that of a continuous (i.e. unjointed) specimen which is otherwise identical.]

Before conducting experiments to investigate the damping properties of a joint with a visco-elastic interfacial layer, damping measurements were carried out on a conventional joint of identical configuration (i.e. as shown in Figure 7a).

The accelerometer measurements were taken in order to obtain the inertia forces applied to the joint. A check was made to ensure that the accelerometer signals were in phase with each other. This was found to be so. The corresponding velocity transducer reading was taken and, in addition, measurements were made of the phase relationship between the velocity at the base of the bar and that across the joint. The sine of the phase angle was obtained using the technique described in Reference 6. With these measurements the energy dissipated was estimated. The experiment was carried out over a range of load amplitudes and repeated with different end masses. The results for the two frequencies are shown in Figure 11, where the energy dissipated per cycle + (joint load)² is plotted against joint load amplitude.

This experiment was then repeated using a joint with a visco-elastic layer. A layer thickness of 0.018 inches was chosen. According to rigid plate theory, this would give a maximum value of energy dissipation at a temperature of 30°C when the joint was excited at 240 c/s.

Similar tests to those carried out on the conventional joint were conducted at three temperatures: 21°C, 24.5°C and 30°C. Tests were carried out at each temperature with the different end masses. This enabled the energy dissipated at the joint to be determined for a range of frequencies. The frequencies examined varied slightly with change in temperature but were approximately 186, 259, 410, 570 and 738 c/s.

It was found that the joint energy dissipation was approximately proportional to the square of the load amplitude over the load range covered. The results had been plotted in Figure 12, 13 and 14 as energy dissipated per cycle \div (joint load)² against excitation frequency at constant temperature.

Using the measured dynamic properties of the visco-elastic material, as obtained in the experiment of § 2 (see Figures 5 and 6), it was possible to predict the energy dissipation from the rigid plate theory. The conditions of temperature and frequency covered in the above experiments have been considered and the theoretical curves obtained from equation (A.3) of the rigid plate theory (see Appendix I) are shown in Figures 12-14.

3.5 Discussion of Results

For the purposes of comparing the energy dissipated in the damped and conventional joints, we shall consider that joint load amplitudes are limited to 50 lb. Above this value, the conventional joint damping is non-linear (this is shown by Figure 11) and the joint itself is fatigue-prone (see § 4). Below the load amplitude of 50 lb, Figure 11 shows that the conventional joint dissipates energy at the rate of $2 \times 10^{-6} \times$ (joint load)² lb in per cycle.

On comparing this value with the measured values plotted on Figures 12-14 it is evident that a considerable damping increment has been obtained by adding a visco-elastic interface to the joint. The magnitude of this energy dissipation does, however, vary considerably with frequency and temperature.

The energy dissipation increases with increasing temperature, this effect being much greater for frequencies less than about 600 c/s. It is also in this frequency range that the largest damping increments are obtained. At the higher frequencies the damping is of the same order as that obtained from the conventional joint.

At the lowest temperature considered (21°C), the largest damping increment is about 200% whilst at the highest temperature (30°C), this has increased to about 350%.

These values compare favourably with those obtained by Cooper⁽⁷⁾. In tests on tubular specimens, made up of riveted dural sheets with Poly-iso-butylene inserts, he obtained damping increments of up to 200% at frequencies of 24 to 40 c/s.

Figures 12-14 indicate that the measured values of the joint energy dissipation are rather lower than the theoretical predictions for all three temperatures considered. The discrepancy increases with increasing temperature particularly at the highest temperature (30°C). The theoretical and experimental values do, however, exhibit similar trends with increasing frequency.

A reduction in the effective shear stiffness of the layer due to incomplete bonding with the joint plates could account for the measured values being generally lower than those predicted theoretically.

In the experiment to determine the dynamic shear modulus, the material properties changed rapidly with change of temperature in the region 26° to 30°C. It would appear, therefore, that errors in measuring the dynamic properties in this region or small errors in temperature measurements in either experiment, could result in appreciable errors in the theoretical curve of Figure 14.

If the curve smoothing associated with the Method of Reduced Variables (8) had been applied to the loss factor curves, then the theoretical curves of Figures 12-14 would exhibit a more marked downward trend at the higher frequencies and would thus agree more closely with the measured values.

There were, therefore, considerable sources of experimental error in this investigation which could account for the discrepancies between the experimental and theoretical values.

4. Fatigue Tests on Simple Riveted Lap Joints with and without a Damping Layer

4.1 Introduction

The introduction of a damping layer into a riveted joint must affect the joint fatigue life under longitudinal loading for several reasons:

- (i) by eliminating the 'friction' load path between the two joint plates, and by providing a 'shear' load path through the damping layer
- (ii) by eliminating fretting between the two inner surfaces of the joint plates
- (iii) by lengthening the rivet shank and so introducing the possibility of bending the rivet

(ii) must increase the fatigue life of the joint; (iii) must tend to reduce it, whereas (i) might affect it either way.

It is evidently desirable to conduct fatigue tests on such joints to obtain experimental evidence of the total effect. The fatigue characteristics of the damping layer itself must also be studied, for failure of the layer destroys its damping effectiveness, weakens the joint fatigue resistance and increases the resonant loads. These, in turn, precipitate more rapid fatigue failure on the whole joint. The fatigue strength of the damping layer must therefore be proved to be satisfactory.

There are many different variables to consider when testing damped joints, e.g. rivet size, joint plate dimensions, type and thickness of the damping layer. Different loading conditions should also be considered.

A comprehensive investigation involving even a few of these variables can only be undertaken as a long term project. The object of the limited series described in this section was to obtain a simple qualitative picture of the fatigue characteristics of damped joints.

Two sets of joints were tested, having joint plate and rivet dimensions identical to those used in the damping measurements of § 3. The first set to be tested had no damping layers. The second had a thick damping layer of about one half the plate gauge. In each case simple harmonic loads were applied at constant amplitude. A suitable range of load amplitudes was covered so that 'S-N' curves could be plotted. From a comparison of these curves it was possible to draw some conclusions concerning the effect of the damping layer on the joint fatigue life. The type of fatigue damage found in these tests has provided useful information concerning the fatigue of such joints.

4.2 The Fatigue Tests Apparatus.

4.2.1 The Fatigue Test Rig

The apparatus used is shown in Figure 15. A horizontal beam was virtually simply supported at its ends and was excited at the resonant frequency of the fundamental flexural mode by an electro-magnetic vibration exciter coupled to the beam centre. The test specimen was inserted to form an integral part of one of the supports, and so was subjected to the beam inertia forces. The damping in the system was kept as low as possible so that a high magnification of the exciting force could be obtained. Thus high longitudinal harmonic loads could be applied to the specimen.

The beam which was manufactured from 2 inch x 2 inch x 18 inch aluminium alloy bar, was attached to the right hand channel section support by a vertical flex-plate. A similar flex-plate was used to attach the beam to the left hand support. This support consisted of a hollow light alloy bar, square in cross section. The specimen lap joint was positioned at the lower end of this bar and was gripped by two jaws, the upper one of which was bolted to the hollow bar, whilst the lower one was firmly bolted to the rig base. Considerable care was taken in the vertical alignment of these jaws, to ensure that the line of action of the loading of the joint lay in the plane of the vertical flex-plate supporting the horizontal beam.

The rigid channel section members on the left of this support provided a reaction to moments and horizontal loads. The top horizontal flex-plate maintained the lateral position of the simply supported beam. The other two horizontal flex-plates were suitably positioned to prevent any bending moments being applied to the specimen. With these precautions bending strains imparted to the specimen were kept to a minimum.

The load was applied to the test specimen mainly by friction due to the pressure of the tightened jaw bolts. It is doubtful whether very much of the axial load was transmitted by the bolts in shear.

The distance between the two jaws was chosen to enable joints with different overlap lengths to be tested, if required. The width of the joint, the plate gauge and the insert thickness could also be varied. Specially machined packing pieces would then be used in order to maintain the alignment of the system. By extending the height of the packing pieces above the level of the jaws and damping them (as shown in Figure 15) joint dynamic buckling loads could be increased above the test load level.

The rig base was rigidly bolted to a bed plate on a heavy concrete block. The fatigue rig was also enclosed in a thick-walled wooden box during tests to reduce the noise radiated into the laboratory.

4.2.2 Maintaining a Constant Test Load on the Joint

It was difficult to maintain a constant load on the joint using the usual system of excitation, viz. an oscillator, power amplifier and vibration exciter. The damping of the beam system was light, and the joint stiffness tended to vary with duration

of loading. Consequently, if the beam was excited at a constant frequency, initially at resonance, the change of joint stiffness was sufficient to throw the system 'off-tune' and so to change the joint load. It was therefore desirable to employ some form of self-excited system which would maintain the oscillation at the varying resonant frequency.

A line diagram, indicating the main features of the system that was used, is shown in Figure 16. This system maintained a constant force amplitude applied to the beam at the natural frequency of the beam, although it would have been preferable to have maintained a constant beam acceleration amplitude. A non-linear resistance bridge incorporating a suitable thermistor element was coupled with a variable ratio transformer. This system provided a negative feed-back voltage proportional to the output voltage of the power amplifier supplying current to the vibration exciter. A positive feed-back voltage proportional to the beam response was obtained from an accelerometer attached to the beam. These two signals could be added and the nett resultant voltage controlled the power amplifier output. On switching on, the oscillations would build up rapidly, stabilising at a pre-determined level. This level depended on the proportion of the power amplifier voltage applied to the non-linear bridge. Changes in the output level could be obtained by suitable adjustment of the variable ratio transformer. The load applied to the joint could therefore be adjusted to any required amplitude.

In theory this would enable the joint load to be maintained at constant amplitude, provide the damping did not change and the excitation frequency was always that of resonance. However, whilst maintaining the system in its resonant conditions, the beam (accelerometer) response could vary for a constant force input due to small changes in the joint stiffness and damping. Modifications could have been made to the existing excitation system so that it could be regulated by the beam response (i.e. the accelerometer output). In this way a constant force would be maintained. It was found, in practice, that the variation in the beam response was gradual and could be satisfactorily adjusted by manual control.

4.2.3 Miscellaneous Additional Facilities

Provisions were made for measuring the resonant frequency of the system (and any variation with time) together with the time to failure of the joint.

It was possible to adjust the joint temperature to any required level.

4.2.4. Preparation of the Specimens

Details of the simple lap joints that were tested are given in Figure 17. The specimens were manufactured from commercial light alloy sheet (L.72) and 3/32" diameter L.37 snap headed rivets.

Every care was taken in the preparation of the specimens to ensure that the scatter inherent in this type of fatigue test was kept to a minimum.

The plates were cut out in the direction of the rolling texture of the sheet and each plate was carefully selected to be free from scratches in the region of the joint. The plates were cut and filed to size on a hardened steel template. The finishing file marks were made to lie along the plate edges and a smooth finish was obtained. Each plate was carefully deburred to eliminate extraneous contact areas.

An attempt was made to provide some uniformity in the riveting process. A pneumatic compression riveter was used to form the snap heads at identical pressures. The rivet shanks were cut to identical pre-determined lengths and were fully heat treated, prior to use.

The joint insert was made in the following manner. The joint plate contact areas were first cleaned with Acetone and then coated with a thin layer of the visco-elastic material, about 0.004 inches thick. The plates were placed under infra-red heating lamps for 48 hours for the material to dry out. A thin sheet of the material, about 0.015 inches thick, was also made up and allowed to dry out for a similar period. Suitable pieces of this sheet were then cut out to be placed between the joint plates. A small amount of the material in liquid form was then smeared on to the contact areas. The configuration was then riveted together and the completed joints placed under the lamps for a further period of 4 to 5 days to dry out completely. By suitable adjustments to the compression riveter and to the rivet shank length that was used it was possible to obtain an interface thickness of 0.017 inches \pm 0.0015 inches.

4.3 Calibration of the Rig

In order to determine the magnification factor of the system a frequency response curve was plotted for constant exciter input current, the response being measured with an accelerometer at the beam centre. From these measurements the damping ratio was obtained (0.008) and hence the magnification factor. It was

found that a load of 120 lb r.m.s. could readily be applied to the test specimen.

In order to measure the force applied to the joint, a strain gauge force transducer was inserted in the jaws of the rig. The strain gauges were mounted on a flat plate of similar dimensions to the test specimens. The system was excited at resonance over a range of exciter current amplitudes. Measurements were taken of the force transducer output together with the corresponding beam accelerometer outputs. Using the latter results and knowing the mass distribution of the beam system, it was possible to estimate the total inertia force exerted on the support and force transducer. This was found to be within 5% of the value indicated by the force transducer measurement. It was therefore possible to estimate the load applied during the fatigue tests from the accelerometer outputs. It was found that there was little variation in mode shape with change in the beam displacement amplitude. It was therefore sufficient to measure the output of just one accelerometer in order to determine the load on the joints.

4.4 Test Procedure and Observations

The object of the tests was to establish 'S-N' curves for lap joints of identical dimensions, with and without damping layers.

Inherent scatter is characteristic of fatigue results, due to small variations in joint fabrication, material structure and test conditions. It was therefore necessary to test a number of specimens at each r.m.s. load amplitude.

Care was taken when inserting the joint in the jaws not to pre-stress the joint. The horizontal beam was always raised to the same position prior to insertion with the aid of a small 'jack' mounted on the vibration exciter. However, in tightening up the jaw bolts some pre-stressing must have been imposed on the specimen.

Tests on the ordinary joints were carried out at room temperature. Tests on the joints with the damping layers were carried out at 30°C. At this temperature and on the known frequency of test, the energy dissipated at the joint should have had a maximum value, according to the rigid plate theory of Part I. (See also Appendix I).

Tests were carried out initially on the conventional lap joints. Specimens were tested at different load amplitudes to

obtain an S-N curve, a sufficient number of specimens being tested at each level to encompass the expected 'scatter' of results.

It was found that two types of failure occurred.

- (i) Failure of the rivet in shear at the common surface of the joint plates
- (ii) Failure of a joint plate in tension within the overlap boundary of the plates (see Figure 17).

It was found that joints with type (ii) failure had a life about twelve times longer than those with type (i) failures. Two separate S-N curves can be obtained corresponding to the two types of failure. These results are shown in Figure 18. The curves drawn through the experimental points have been obtained by taking a logarithmic mean of the experimental data at each load level. There was a slightly larger number of failures of plates than of rivets.

A number of phenomena were observed during the course of these tests and are described below.

Whilst the fundamental frequency of the self-excited system differed slightly with each specimen tested and with load amplitude, there was a clear distinction between the excitation frequencies of the sets of specimens with different types of fatigue failure. The system responded initially at a frequency of about 265 c/s when testing specimens which gave type (i) failures, and at about 285 c/s for specimens giving type (ii) failures.

For joints requiring several minutes or more to fail it was possible to follow the variation in the fundamental frequency of the system with time. Tests on joints giving rise to a type (ii) failure showed an increase in the frequency with time. The final increment, achieved in about two minutes, was approximately 2%. For type (i) failures the effect was less apparent, the frequency staying approximately constant. This period was followed by a gradual decrease in the fundamental frequency to a value some 10 c/s below the initial value. The specimen frequency then dropped rapidly as the specimen failed. The gradual decrease in frequency showed no definite pattern, staying at a particular value for a longer period than at others. This pattern differed with each specimen that was examined. A mean value was taken for the fundamental frequency in order to estimate the number of cycles to failure.

An annular area of black aluminium oxide was observed on the plate interfaces around the rivet, due to the fretting action between the faces. Type (i) rivet failures generally had very little of this oxide film away from the rivet hole. In the case of plate failures the oxide film was found to extend over a large annular area up to $\frac{1}{4}$ inch in diameter.

Some local crazing of the outer surface of the joint plates was observed inside the overlap (see Figure 17). Plate fatigue cracks were always located in this region. On carrying out a metallurgical investigation it was found that a large number of slip bands had been generated producing the 'orange peel' effect visible to the naked eye.

Tests carried out on joints with a damping layer produced, in general, similar phenomena. Again, the two types of joint failure were observed. The S-N curves obtained are shown in Figure 19. These indicated a longer fatigue life for this type of joint, particularly for specimens subject to rivet failure (about ten times). Only about a third of the specimens tests produced rivet failures. This time there was no initial rise in frequency, but a gradual haphazard decrease in the fundamental frequency was observed. The magnitude of the total drop depended on the life of the specimen and was as great as 25 c/s. A rapid drop in frequency occurred at failure. Again a mean value for the frequency was taken in assessing the number of cycles to failure.

The only evidence of fretting appeared to be due to rubbing of the rivet shank against the edges of the rivet hole. There did not appear to be any fatigue failures of the damping layer.

4.5 Discussion of Results

The experimental observations suggest that the two types of failure that occur depend on the forming of the rivet.

The two distinct regions of excitation frequency corresponding to the two types of failure indicate that the joints concerned are of different stiffness. For the conventional joints, this would appear to depend on the normal pressure set up between the joint plates during the riveting process. Since considerable care was taken to control this parameter when using the compression riveter this variation could well occur in a practical case.

For a well formed rivet the adjacent surfaces of the plates would be pressed tightly together and the asperities would be deeply embedded in the opposite surface. In the case of a joint

where the rivet forming resulted in a lower normal pressure, the contact between the joint plates would not be so great. The stiffness of the joint and the capacity of the joint plates to transmit part of the joint load in shear would therefore be reduced. Thus the rivet would be subjected to a greater dynamic loading and would therefore be more susceptible to fatigue.

The nature of the fretting supports this hypothesis. In the case of plate failures the larger fretting areas indicate greater dynamic friction between the joint plates than in the case of those with rivet failures.

The initial rise in frequency with joints subject to plate failure corresponds to an initial increase in joint stiffness. This is probably due to some of the aluminium oxide deposit causing the rivet to 'seize-up' in its hole. The gradual drop in frequency corresponds to a reduction in joint stiffness, and is probably due to fatigue occurring on a microscopic scale, perhaps from the initial load cycle onwards. Eventually the fatigue failure concentrates the load path sufficiently to bring about a rapid failure with a corresponding reduction in excitation frequency.

The smaller number of rivet failures and the improved rivet life in joints with a damping layer would suggest that the rivets are subjected to a lower loading than the corresponding specimens in the conventional joint.

Most of the plate failures occurred close to the rivet. In Appendix II the load in the plate at the rivet has been assessed from the rigid plate theory of Part I (see Appendix I) assuming optimum conditions for the plate configuration (optimum conditions were approached in the test, as near as was possible). The load in the plate has been estimated from this analysis to be 0.76 of the applied load. Thus the load in the plate at this point is 0.76 of that in the conventional joint for the same joint load. In theory, therefore, the S-N curves for the plate failures of the two types of joint should coincide if the conventional joint load scale is factored by 0.76. This factored curve is shown in Figure 19. The two curves do, in fact, correspond quite well. The required factor is, however, about 0.8. Considering the assumptions and possible sources of error this is a very good agreement.

The gradual fatiguing process indicated by the gradual frequency drop again occurred in the specimens with a visco-elastic layer.

The reason for the 'orange peel' stress concentration close to the rivet has not been fully explained. It is probably due to the presence of the rivet combined with some bending of the plate.

It can be said that, within the limits imposed in this fatigue investigation, the presence of the damping layer improved the fatigue life of the riveted joint. A more comprehensive investigation on the lines suggested in § 4.1 is, however, necessary before such joints could be used in an aircraft structure.

5. Conclusions

An experiment was conducted to measure the complex shear modulus of the damping layer material (Polyvinyl Acetate) over a temperature range of 12 to 30 degrees Centigrade, and a frequency range of 100 to 1000 c/s. The results were used to predict a suitable layer thickness and also to compare the theoretical predictions of Part I⁽¹⁾ with measured values of the joint energy dissipation. The real part of the complex shear modulus increased rapidly with increasing frequency or decreasing temperature. The corresponding curves for the material loss factor did not behave in a simple fashion. Whilst there were no sharp discontinuities with frequency variation, rapid changes were observed with variation in temperature. This was particularly noticeable at the higher temperatures considered. At temperatures below average room conditions the loss factor decreased markedly with frequency. Similar marked variations in loss factor have been observed by other experimenters. There was however some indication that the measuring equipment was insufficiently sensitive for the conditions existing at the higher temperatures.

Measurements of the damping were carried out on joints with and without damping layers. It was found that considerable damping increments could be obtained by the addition of the layer. However, the magnitude of the energy dissipations varied considerably with frequency and temperature due to the changes in the dynamic properties of the material. Damping increments of up to 350% were obtained, these values comparing favourably with those measured by Cooper⁽⁷⁾ in tests on a riveted tubular specimen.

The measured values of the joint energy dissipation were lower than theoretical predictions, particularly at the highest temperature considered (30°C). The theoretical and experimental curves did however exhibit similar trends with frequency variation. These discrepancies might be accounted for by incomplete bonding

between the damping layer and the joint plates, together with the possible errors in measurement of the complex shear modulus.

Fatigue tests carried out on riveted joints with and without a damping layer indicated that, within the limits imposed during the test, the presence of the layer improved the fatigue life of the joints.

The joints were subjected to simply harmonic axial loading at constant amplitude. A range of load amplitudes were investigated. Two 'S-N' curves were found for each type of specimen corresponding to two types of failure, viz:

- (i) Failure of the rivet in shear at the joint plate interface.
- (ii) Failure of a joint in tension within the overlap boundary of the plates.

The type of failure in the conventional riveted joints appeared to depend on the normal pressure between the joint plates. If the rivet was well-formed, the adjacent surfaces of the plates were pressed tightly together. If the rivet was poorly formed the pressure between the joint plates would not be so great, and the capacity of the plates to transmit part of the joint load in friction would be considerably reduced. The rivet would therefore be subjected to a greater load and would therefore be more susceptible to fatigue.

The nature of the fretting and the stiffness variation of the tested joints substantiated this hypothesis.

The small number of rivet failures and the improved fatigue life in joints with a damping layer indicated that the layer was transmitting a greater proportion of the load than that transmitted by friction in a conventional joint. A simple analysis based on rigid plate theory suggested that the load in the plates at the rivet was less in the damped joint than in the conventional joint. This would increase the plate fatigue life and was found to be so in the experiment.

In Part I the potentialities of joint damping layers for increasing structural damping were discussed with particular reference to the choice of the most suitable joints for their inclusion. It was concluded that circumferential and longitudinal skin-to-skin joints in fuselages, and the chordwise skin joints in wings were best suited to this treatment.

In general, the experimental investigations confirm that damping layers can produce appreciable damping increments. The

principal problem is likely to be in obtaining a visco-elastic material which will work satisfactorily for a wide range of environmental conditions. In particular, difficulties are likely to arise due to the high temperatures associated with high speed flight. At present the most likely application will be in regions where inserts are already necessary. Skin-to-skin joint sealants are required for integral fuel tanks. In a region of high noise level some weight saving might be obtained by using a sealant which also has appreciable damping properties.

Appendix I - A Summary of the Rigid Plate Theory

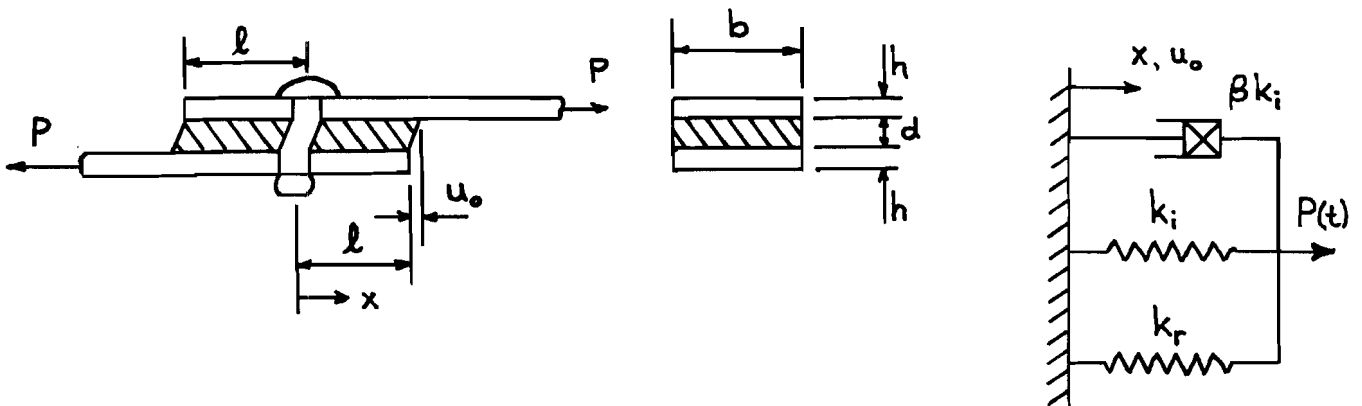
In Part I⁽¹⁾ it was shown that the energy dissipation per load cycle, Δ , in a joint of finite stiffness can be expressed in the form:

$$\Delta = \left\{ \frac{\pi P^2}{Eb} \right\} \cdot f$$

where f is a known complicated function depending on the parameters k_r/Eb , ϕ , l/h and β .

k_r is the rivet stiffness (load per unit deflection) which includes any flexibility due to bearing stress concentration at the rivet location.

$$\phi = \left\{ \frac{2Gh}{Ed} \right\}^{\frac{1}{2}} \text{ and is known as the 'shear parameter'.$$



It has been shown that if the rivet stiffness parameter k_r/Eb is less than 0.003, then the energy dissipated corresponds closely to that of a joint with rigid plates, i.e. $E \rightarrow \infty$. Under these conditions the complex shear force being transmitted at any instant by the rivet and damping layer is:

$$u_0 \left\{ k_r + k_1 (1 + i\beta) \right\} = P \exp(i\omega t) \quad \dots (A.1)$$

$$\text{where } k_1 = \left(\frac{2lb}{d} \right) G = \text{the real part of the shear stiffness of the layer} \quad \dots (A.2)$$

It may be shown that the energy dissipated per load cycle is:

$$\Delta_s = \pi P^2 \beta k_i / \{ (k_r + k_i)^2 + \beta^2 k_i^2 \} \quad \dots (A.3)$$

Normally the rivet stiffness and the dynamic properties of the shear material are known, and an optimum value of the layer stiffness is required which will give the maximum energy dissipation. This optimum occurs when the modulus of the complex shear stiffness of the interface is equal to the rivet stiffness (providing $k_r/Eb < 0.003$), i.e.

$$k_i (1 + \beta^2)^{\frac{1}{2}} = k_r \quad \dots (A.4)$$

Normally, the overlap length, ℓ , is likely to be determined by static strength or manufacturing requirements so that equation A.4 gives the optimum thickness of the layer.

The corresponding energy dissipation, with the given interface material, can be readily obtained by substituting equation A.4 into equation A.3, viz:

$$\Delta_{s_{\max}} = \frac{\pi P^2}{2k_r} \cdot \left\{ \frac{\beta}{(1 + \beta^2)^{\frac{1}{2}} + 1} \right\} \quad \dots (A.5)$$

Appendix II - Theoretical Estimation of the Plate Load at the Rivet in a Joint with a Visco-Elastic Layer

In this analysis the rigid plate theory has been assumed.

From equations A.1 and A.2 in Appendix I it is seen that the relative displacements of the joint plates, u_o , corresponding to a longitudinal harmonic load $P \cdot \exp(i\omega t)$, can be written in the form:

$$u_o = \frac{P \exp(i\omega t)}{k_r + k_i \cdot (1 + i\beta)}$$

Thus the total load passing through the layer of stiffness $k_i \cdot (1 + i\beta)$ must be:

$$P_i = \frac{k_i \cdot (1 + i\beta) P \exp(i\omega t)}{k_r + k_i \cdot (1 + i\beta)}$$

The load in the plate at the rivet is:

$$\begin{aligned} P_p &= P - \frac{P_i}{2} \\ &= \frac{P}{2} \left\{ \frac{2k_r + k_i \cdot (1 + i\beta)}{k_r + k_i \cdot (1 + i\beta)} \right\} \end{aligned}$$

The modulus of this is:

$$\begin{aligned} |P_p| &= \frac{P}{2} \left\{ \frac{(2k_r + k_i)^2 + (k_i \beta)^2}{(k_r + k_i)^2 + (k_i \beta)^2} \right\}^{\frac{1}{2}} \\ &= \frac{P}{2} \left\{ \frac{(2 + k_i/k_r)^2 + (k_i/k_r)^2 \beta^2}{(1 + k_i/k_r)^2 + (k_i/k_r)^2 \beta^2} \right\}^{\frac{1}{2}} \end{aligned}$$

Now optimum properties for a given joint configuration are given by equation A.4, viz:

$$k_{i_{opt}} = k_r / (1 + \beta^2)^{\frac{1}{2}}$$

Assuming that the temperature and frequency are such that the layer has the optimum properties, then the plate load becomes

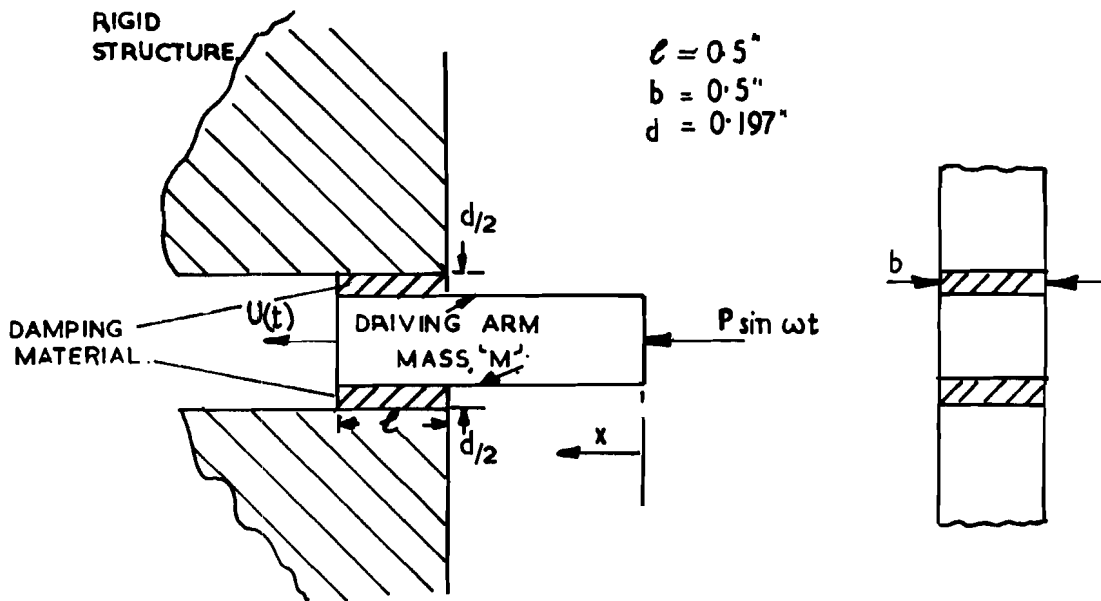
$$|P_p| = \frac{P}{2} \left\{ \frac{(2(1 + \beta^2)^{\frac{1}{2}} + 1)^2 + \beta^2}{((1 + \beta^2)^{\frac{1}{2}} + 1)^2 + \beta^2} \right\}^{\frac{1}{2}}$$

In the practical case considered in § 4, $\beta = 1.5$. We have, therefore, for this case:

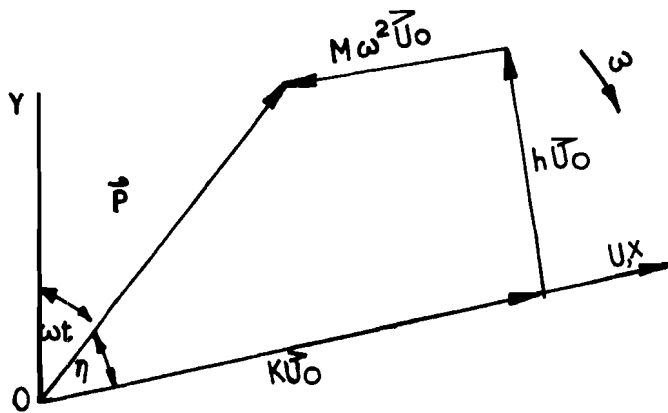
$$P_p = 0.762P$$

R E F E R E N C E S

1. Mead, D.J.
Eaton, D.C.G. 'Interface Damping at Riveted Joints.
Part I - Theoretical Analysis'
ASD Technical Report 61-467 Part I.
2. Ed. Eirich, F.R. 'Rheology - Theory and Applications'
Academic Press Inc., New York
3. Ferry, J.D. 'Mechanical Properties of Substances
of High Molecular Weight'
Journal of the American Chemical
Society Vol.72, p.3746 (1950)
4. Nolle, A.W. 'Dynamic Mechanical Properties of
Rubberlike Materials'
5. Mead, D.J. 'The Internal Damping due to Structural
Joints and Techniques for General
Damping Measurements'
Aeronautical Research Council Current
Paper, No.452, H.M.S.O. London (1959)
6. Mead, D.J. 'The Effect of a Damping Compound on
Jet Efflux Excited Vibrations.
Part I - Structural Damping due to the
Compound'
Aircraft Engineering Vol.32, No.373
7. Cooper, D.H.D. 'A Suggested Method of Increasing the
Damping of Aircraft Structures'
Aeronautical Research Council Reports
and Memoranda 2398, H.M.S.O. London
(1959)



1a. LINE DIAGRAM OF THE CONFIGURATION SHOWING THE GEOMETRY AND THE SYSTEM OF CO-ORDINATES.



1b. VECTOR DIAGRAM OF THE FORCES SET-UP DURING EXCITATION.

FIGURE 1. MEASUREMENT OF THE COMPLEX SHEAR MODULUS:
THE CONFIGURATION AND THE DYNAMIC EQUILIBRIUM OF FORCES.

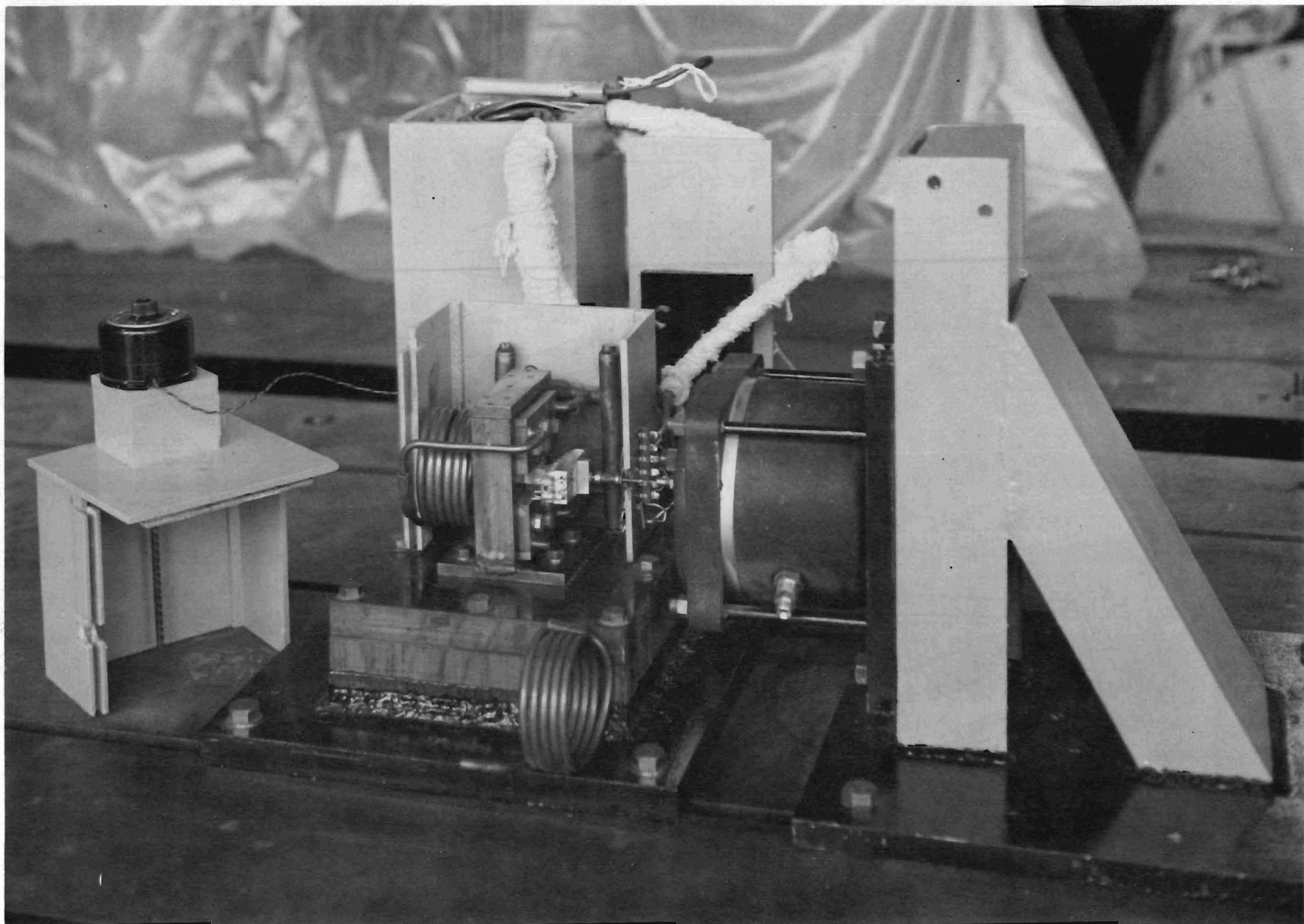


FIGURE 2 APPARATUS FOR MEASURING THE COMPLEX SHEAR MODULUS OF VISCO-ELASTIC MATERIALS- GENERAL VIEW.

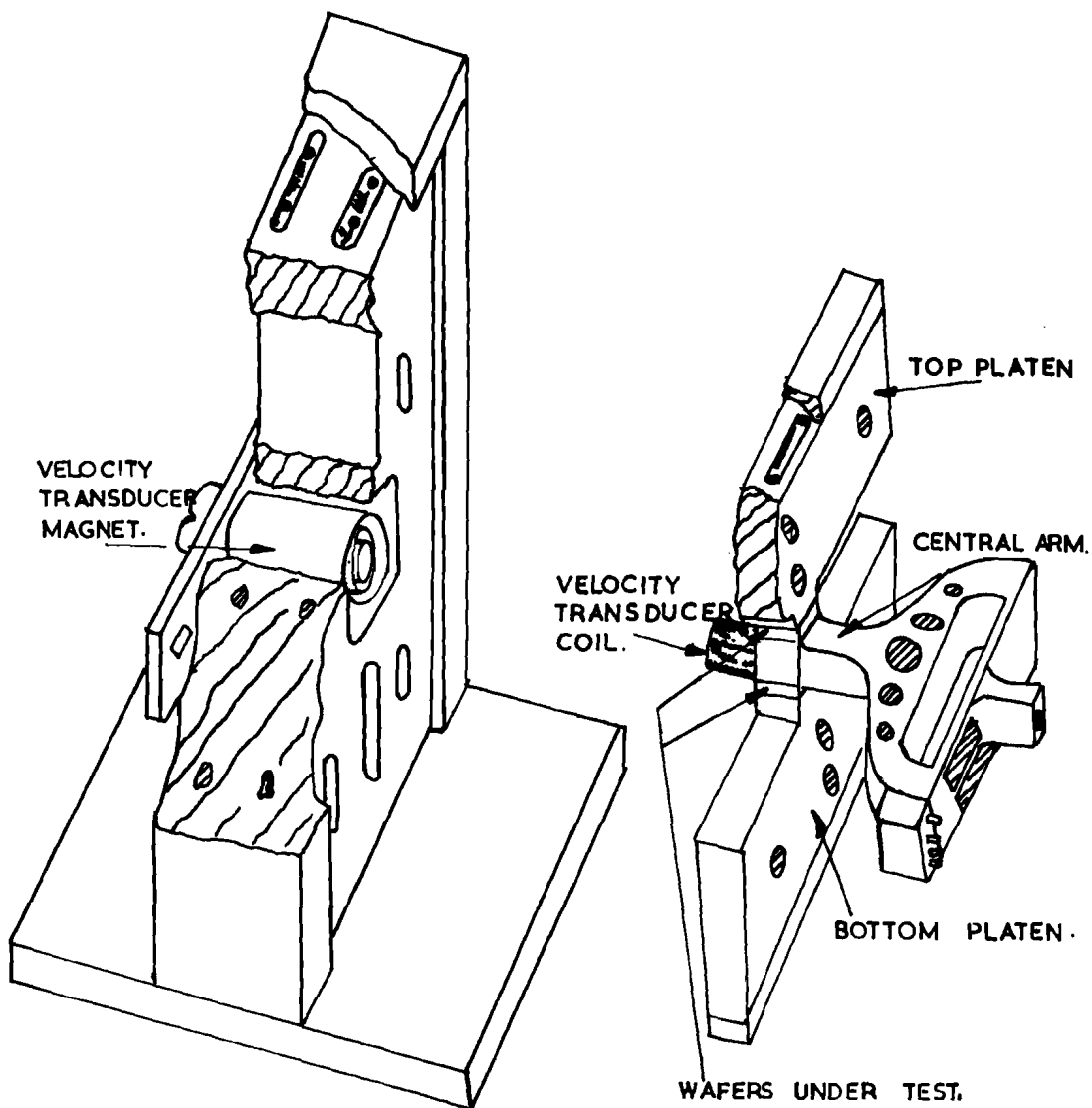


FIGURE 3. APPARATUS FOR MEASURING THE COMPLEX SHEAR MODULUS OF VISCO-ELASTIC MATERIALS: 'EXPLODED' VIEW.

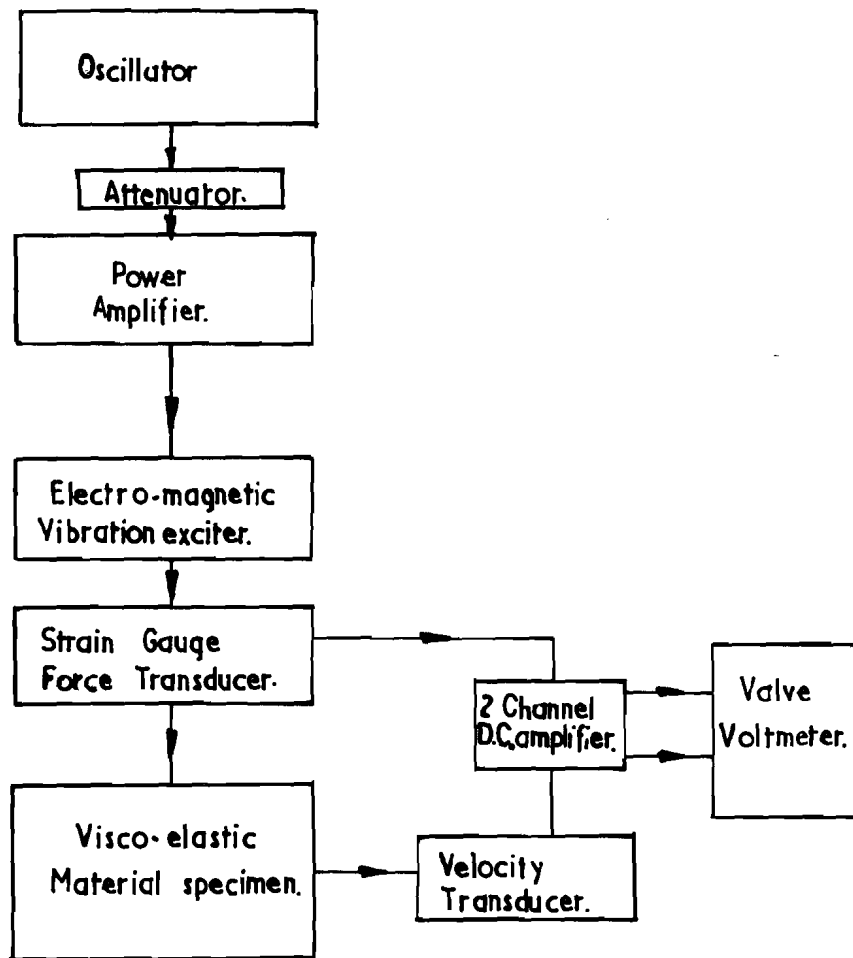


FIGURE 4. BLOCK DIAGRAM OF THE EXCITING AND MEASURING SYSTEMS.
COMPLEX SHEAR MODULUS APPARATUS.

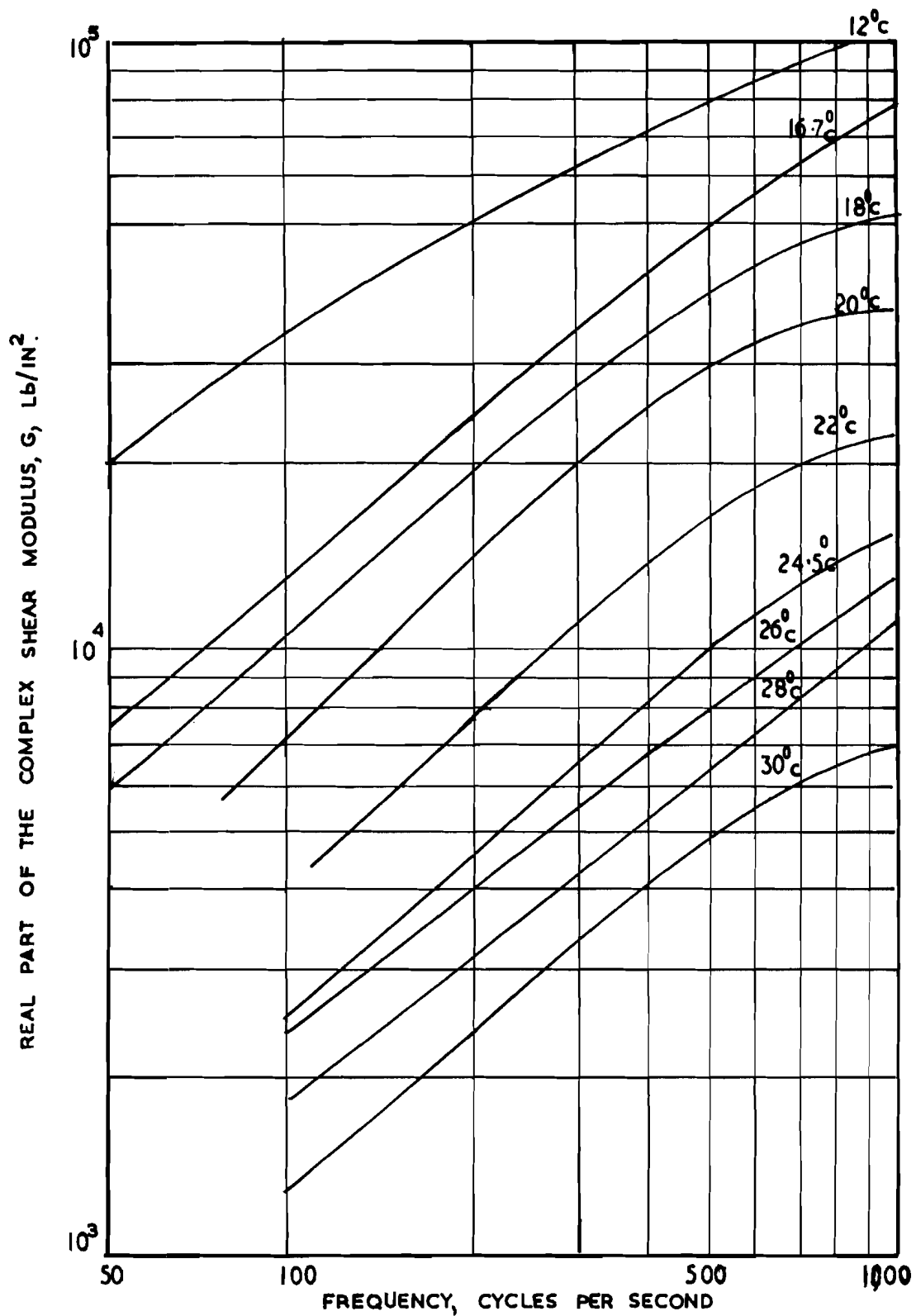


FIGURE 5. VARIATION WITH FREQUENCY AND TEMPERATURE OF THE REAL PART OF THE COMPLEX SHEAR MODULUS.

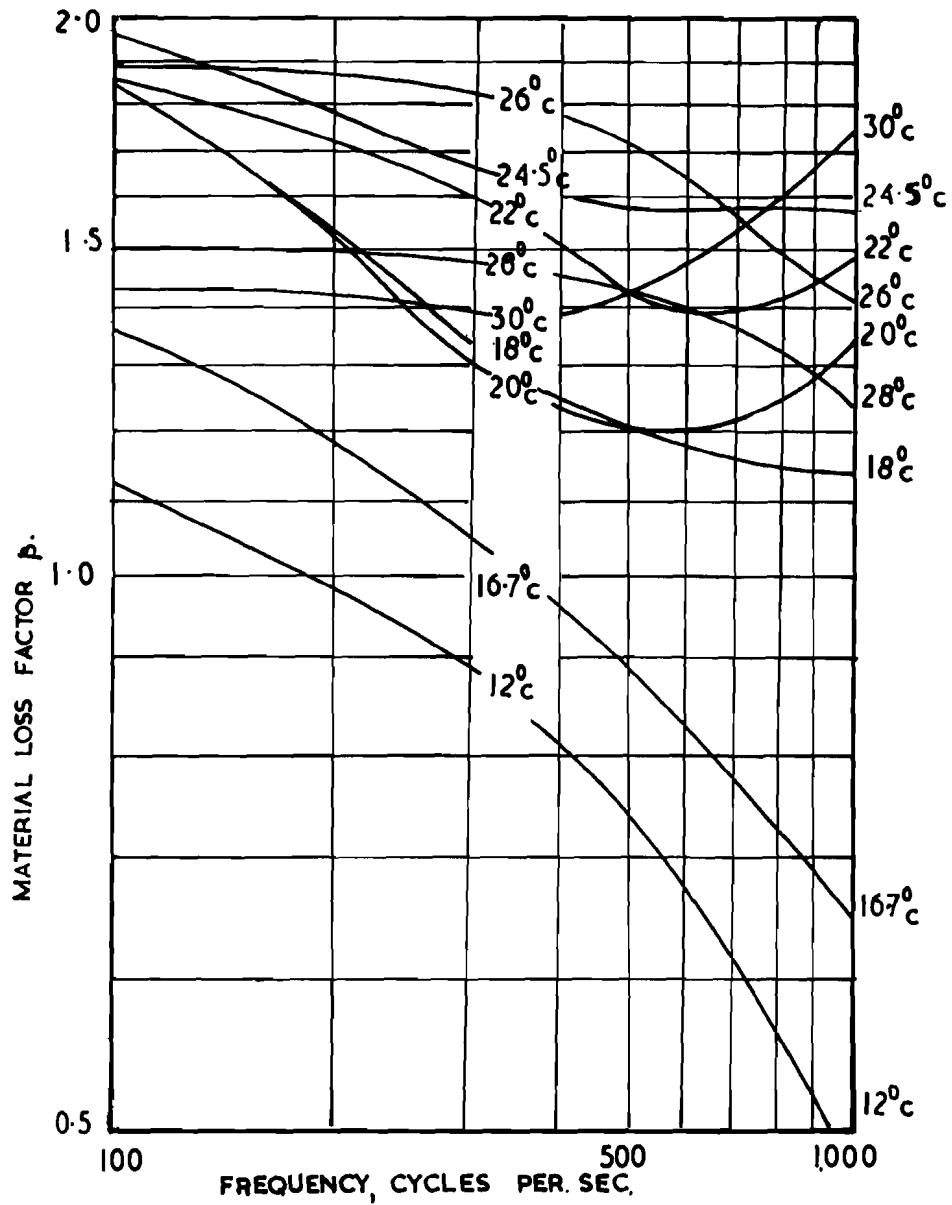


FIGURE 6 VARIATION WITH FREQUENCY AND TEMPERATURE OF THE MATERIAL LOSS FACTOR.

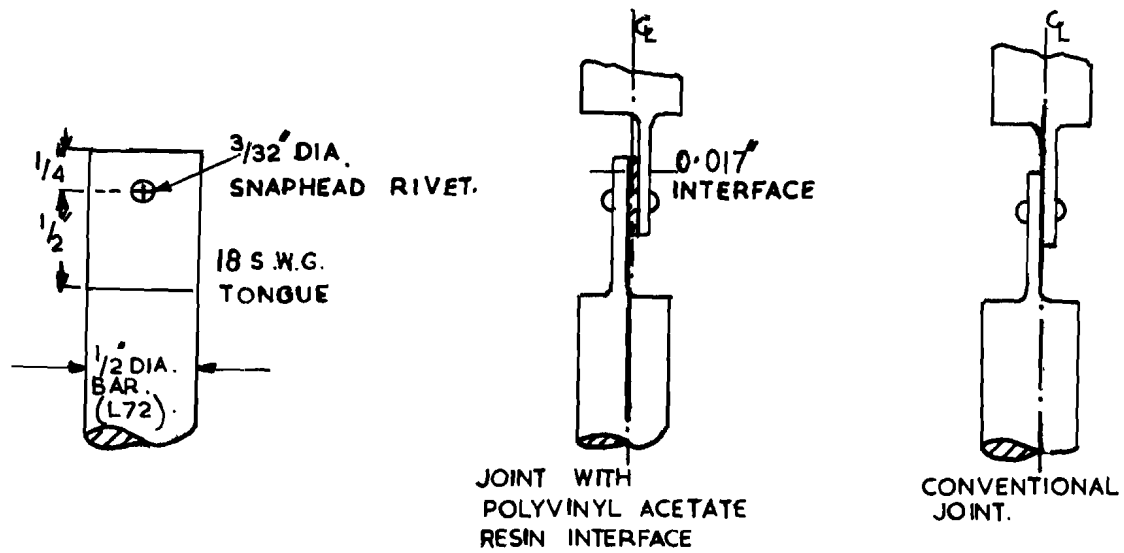


FIGURE 7a DETAILS OF JOINTS FOR DAMPING MEASUREMENTS.

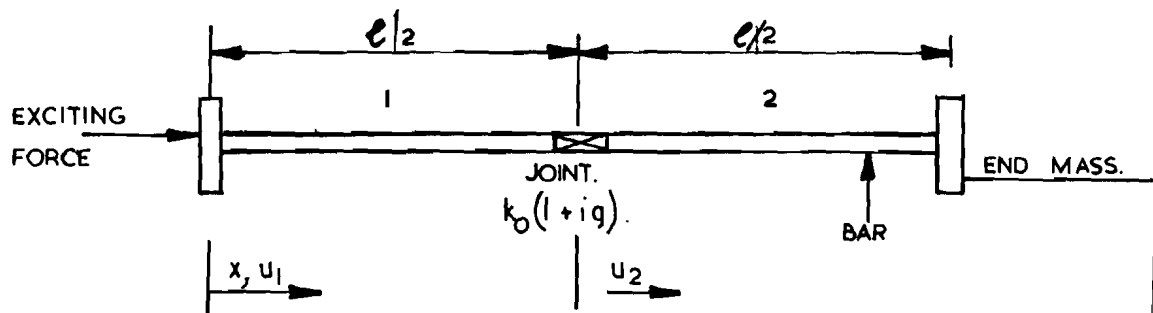


FIGURE 7b. DIAGRAM OF THE BAR WITH JOINT.

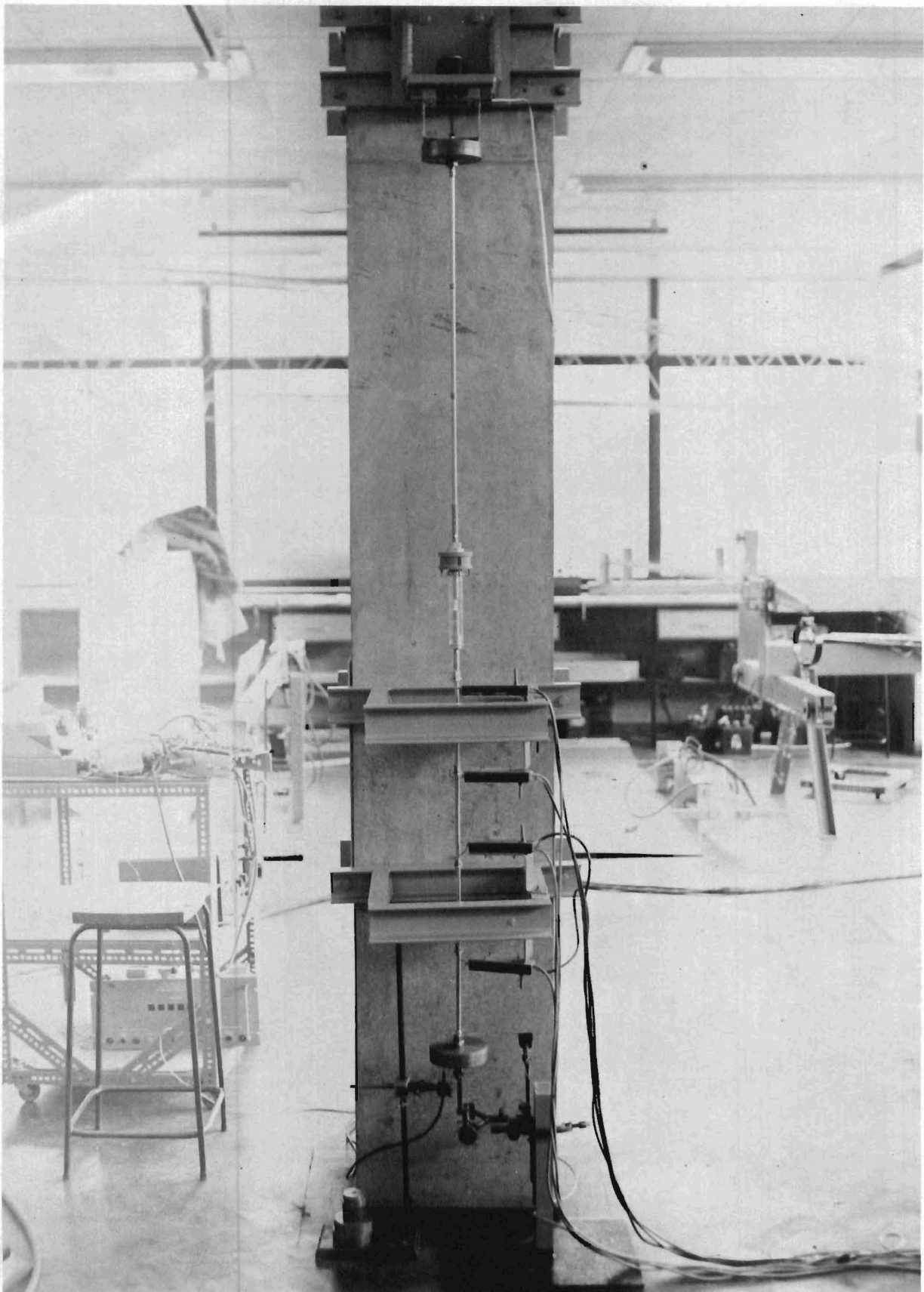


FIGURE 8. APPARATUS FOR MEASURING THE STIFFNESS AND DAMPING OF A RIVETED JOINT WITH A DAMPING LAYER.-GENERAL VIEW

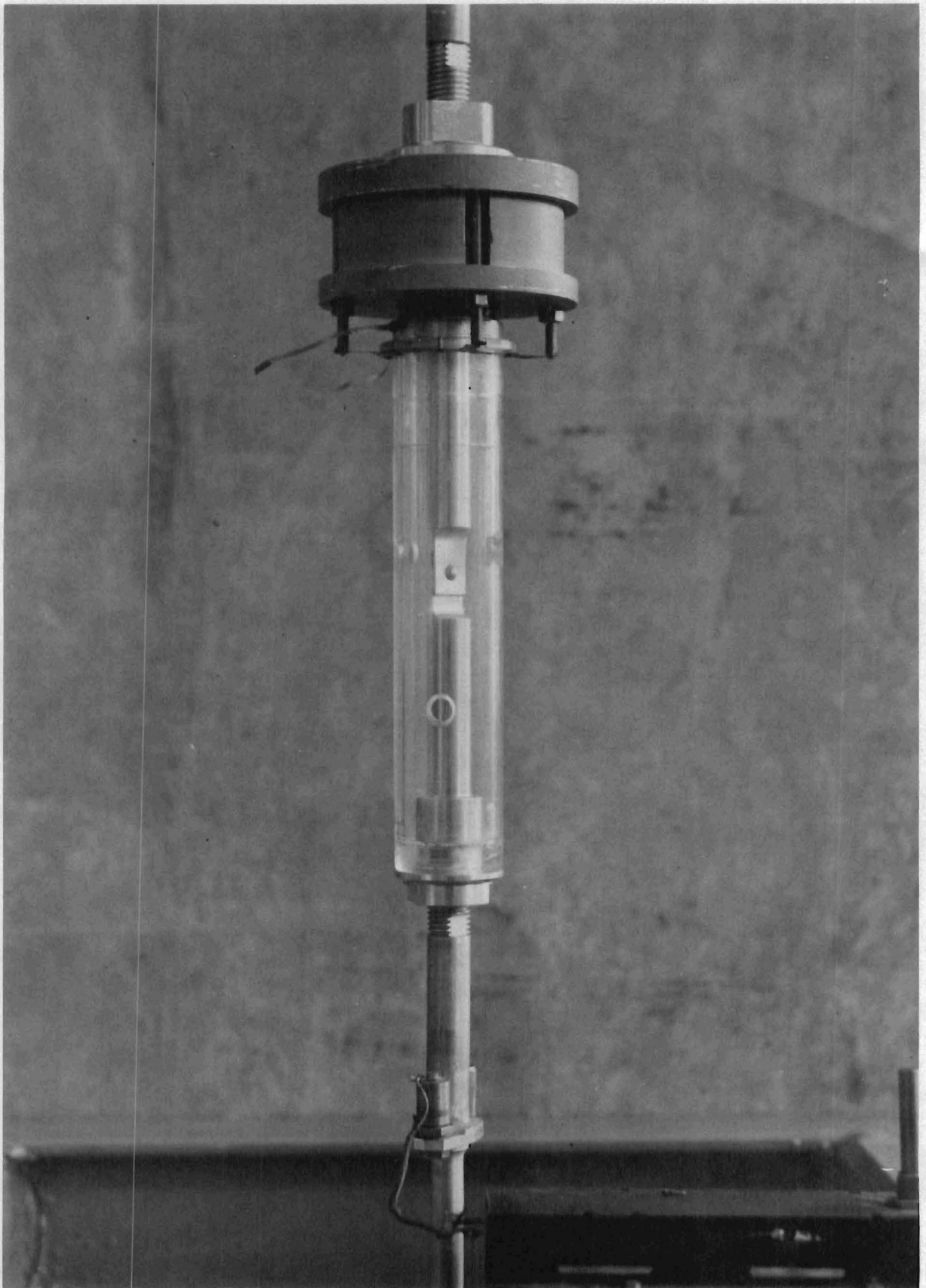


FIGURE 9 . APPARATUS FOR MEASURING THE STIFFNESS AND DAMPING OF A RIVETED JOINT WITH A DAMPING LAYER - CENTRAL PORTION.

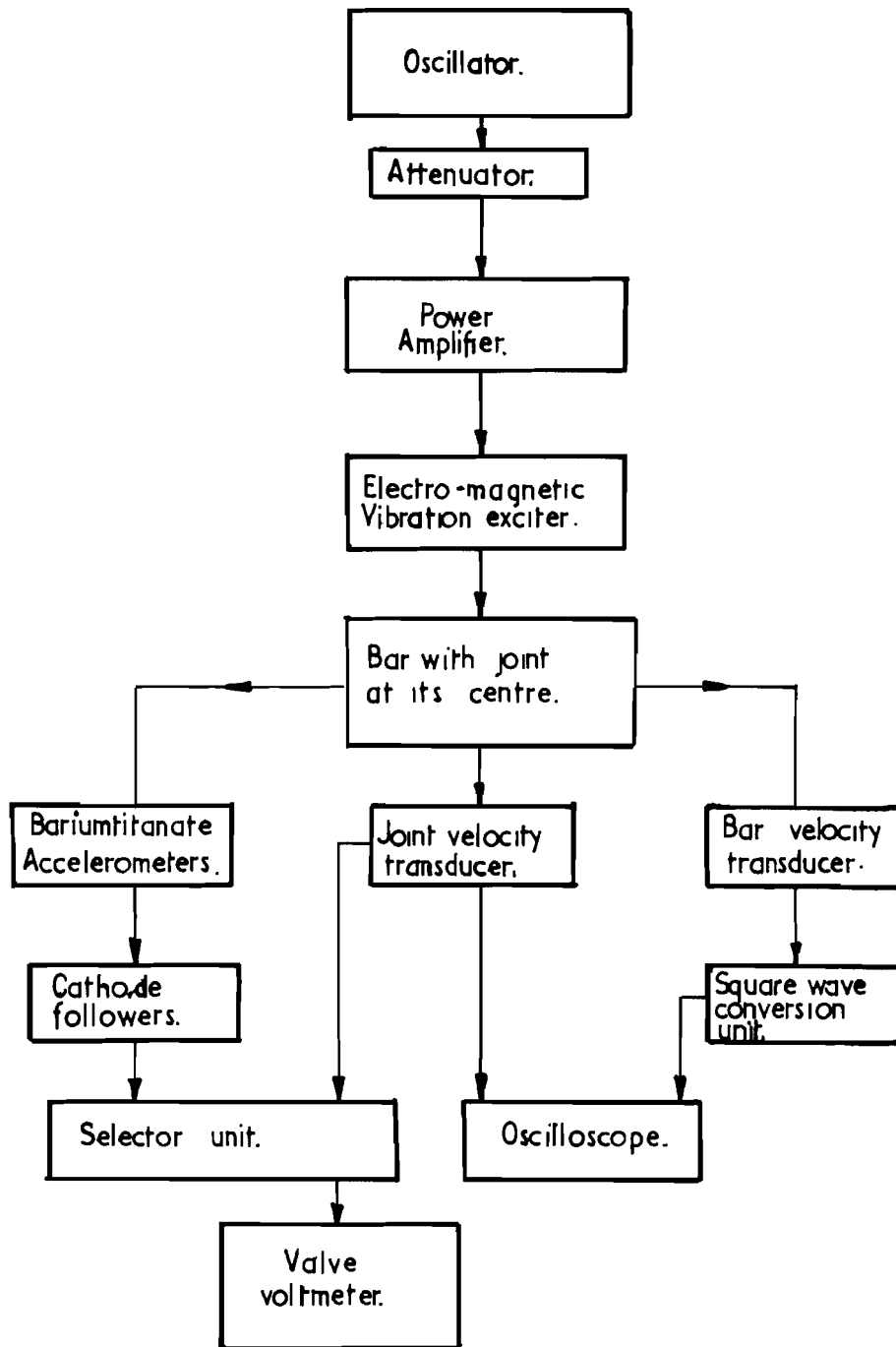


FIGURE 10 BLOCK DIAGRAM OF THE APPARATUS FOR MEASURING THE STIFFNESS AND DAMPING PROPERTIES OF A RIVETED JOINT

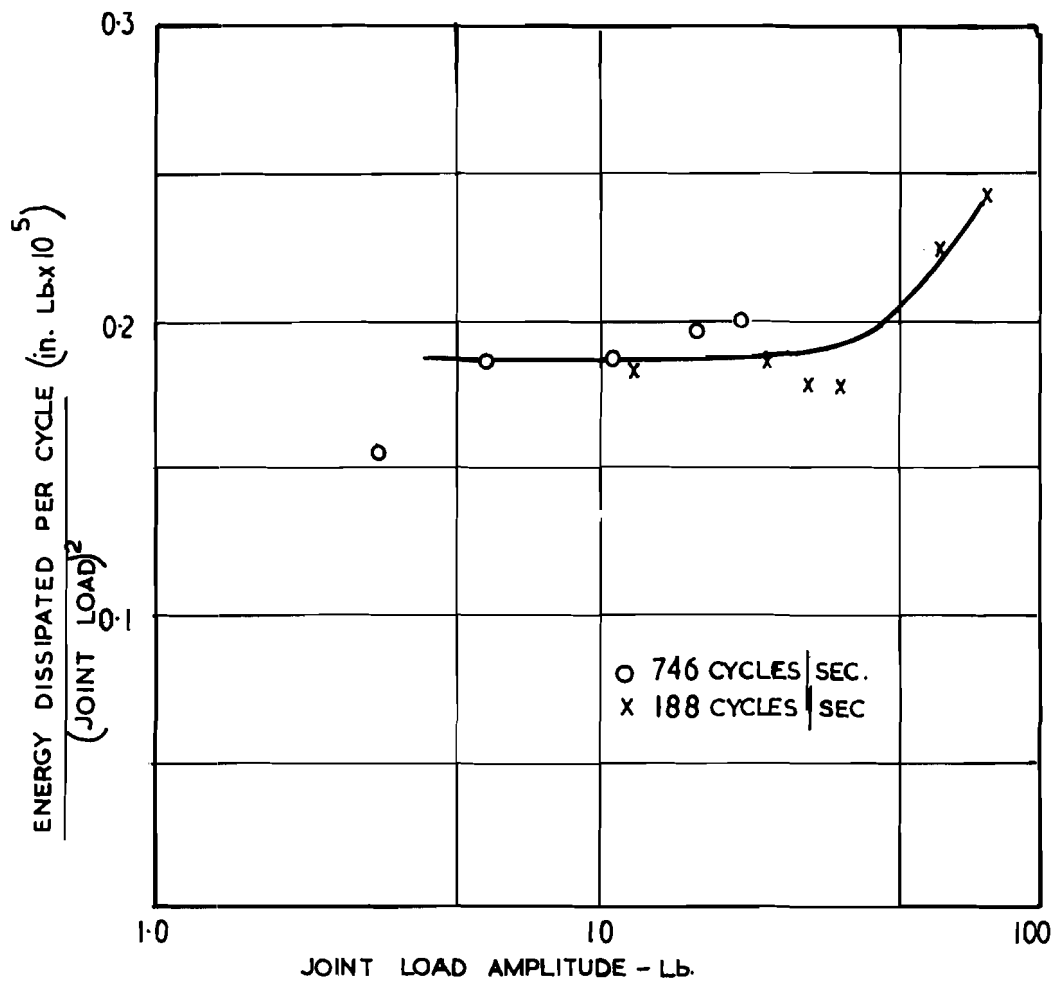


FIGURE II. THE VARIATION WITH LOAD AMPLITUDE OF THE ENERGY DISSIPATED PER CYCLE AT A CONVENTIONAL RIVETED JOINT

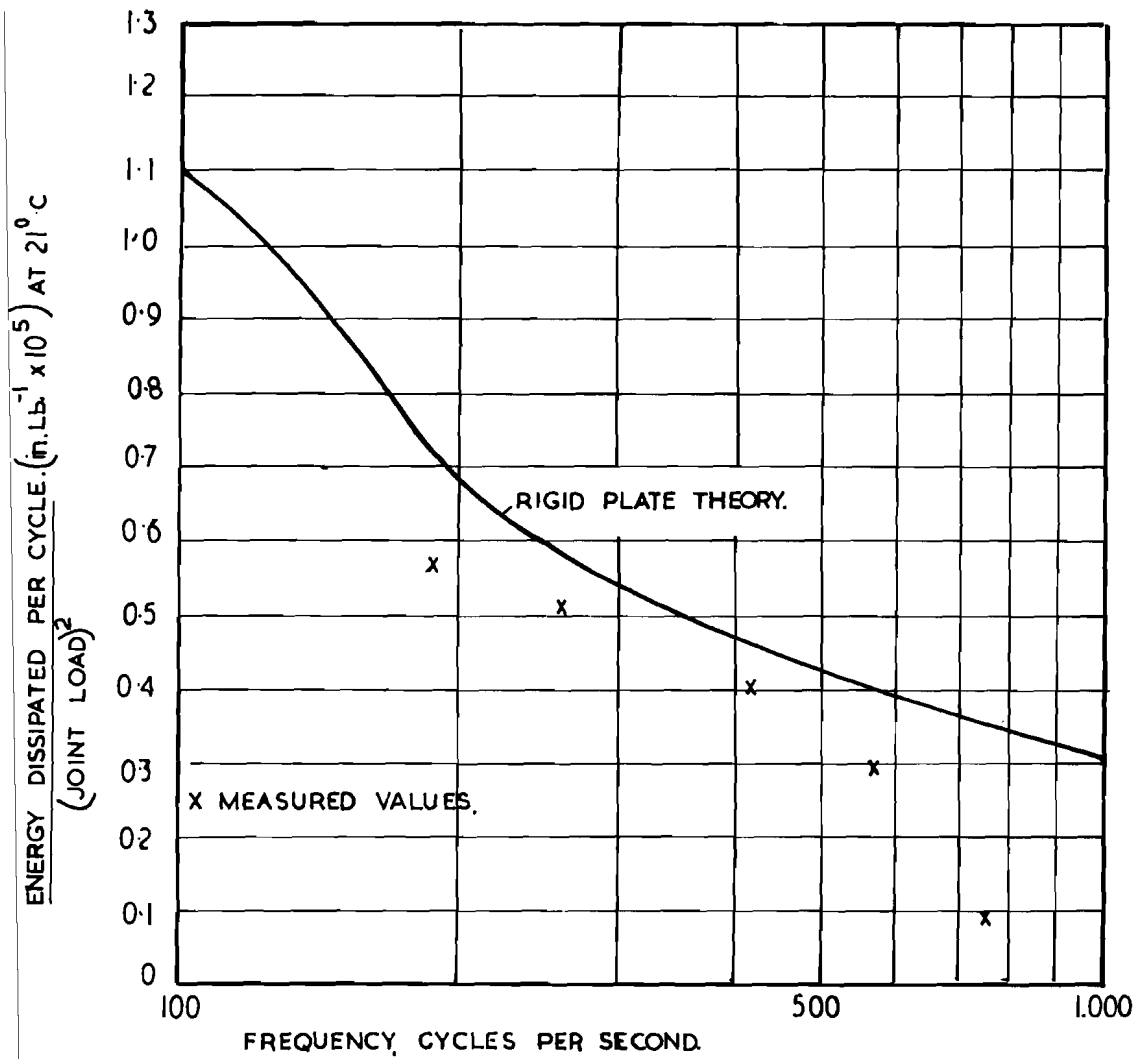


FIGURE 12. THE VARIATION WITH FREQUENCY OF THE ENERGY DISSIPATED PER CYCLE AT A JOINT WITH A VISCO-ELASTIC INTERFACE. JOINT TEMPERATURE - 21°C

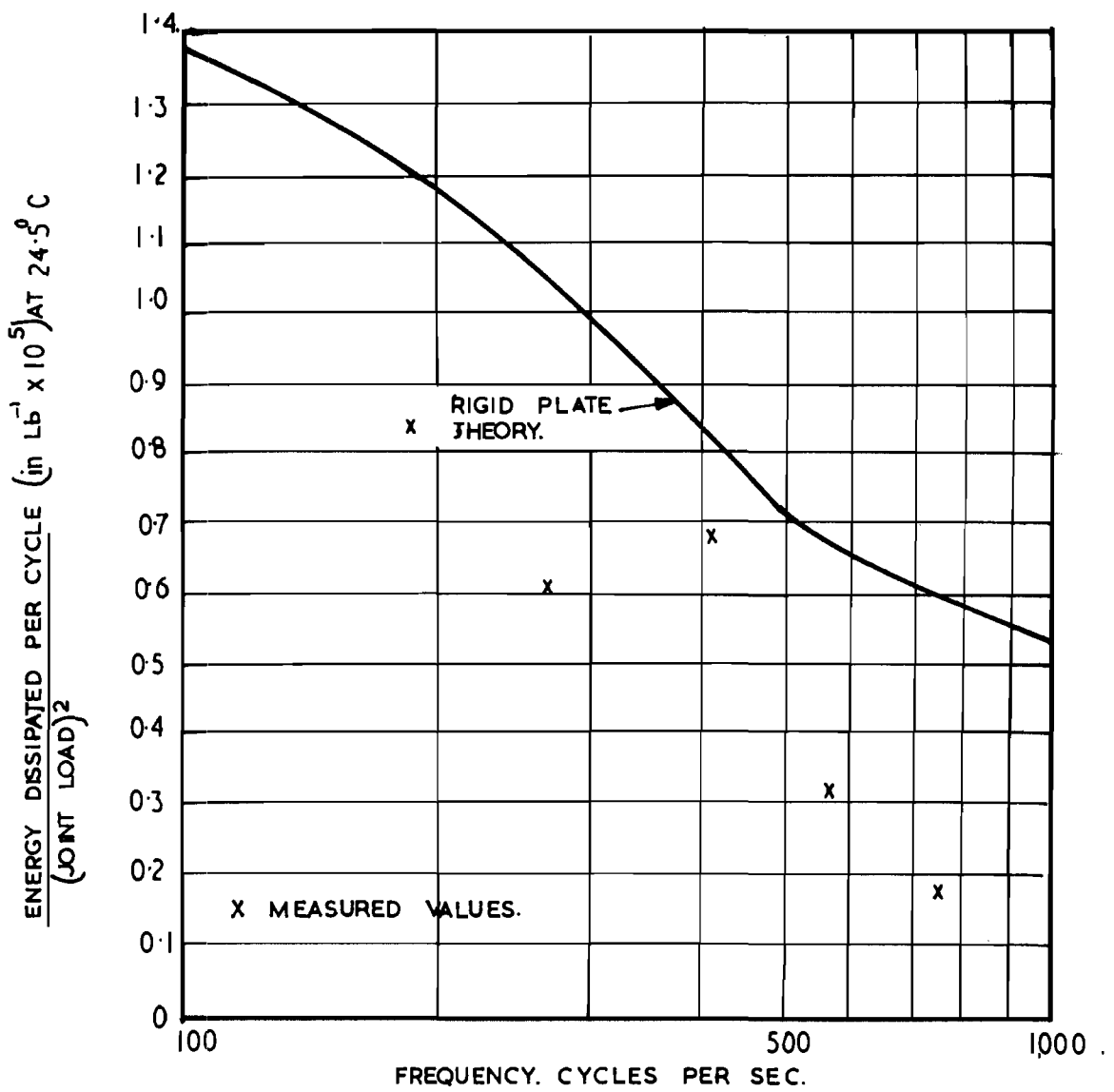


FIGURE 13. THE VARIATION WITH FREQUENCY OF THE ENERGY DISSIPATED PER CYCLE AT A JOINT WITH A VISCO-ELASTIC INTERFACE. JOINT TEMPERATURE = 24.5° C

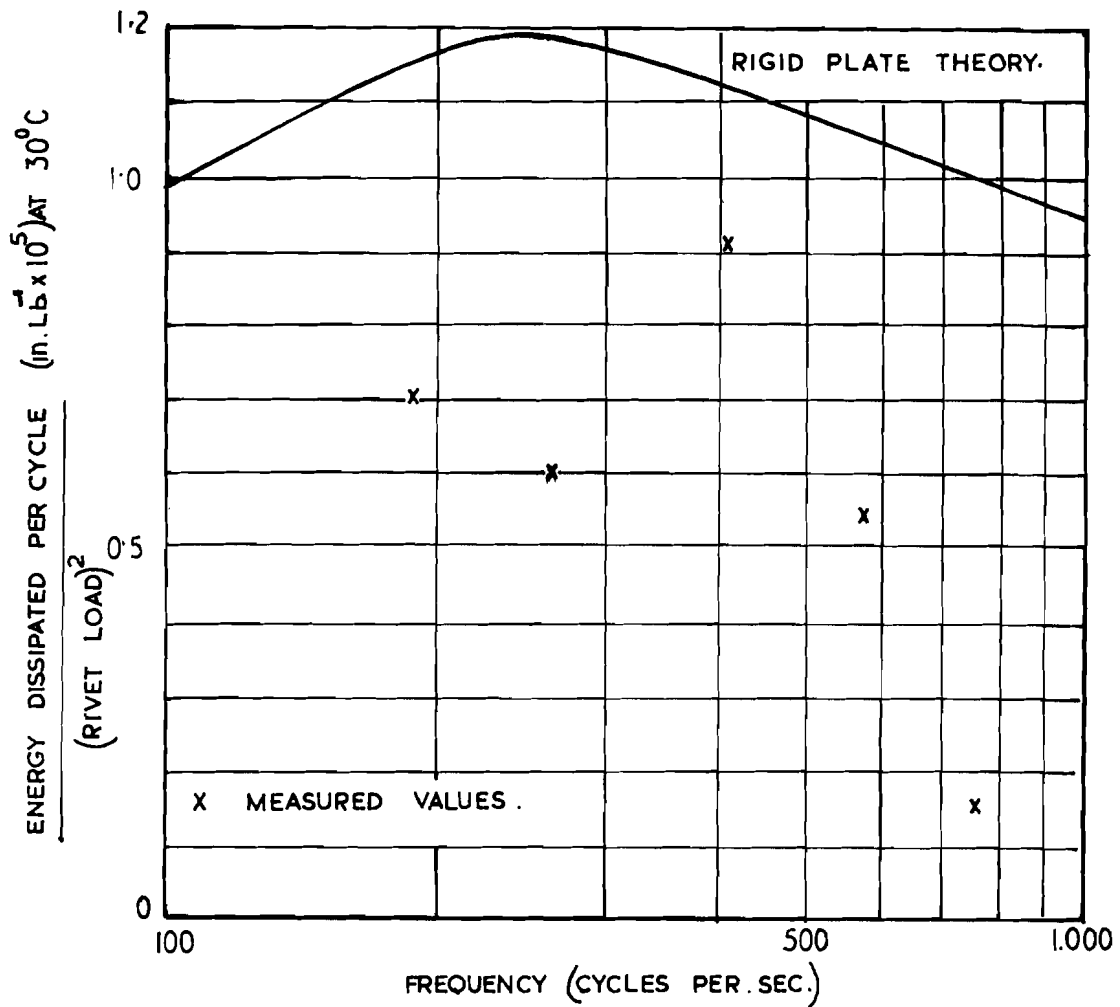


FIGURE 14. THE VARIATION WITH FREQUENCY OF THE ENERGY DISSIPATED PER CYCLE AT A JOINT WITH A VISCO-ELASTIC INTERFACE. JOINT TEMPERATURE = 30° C.

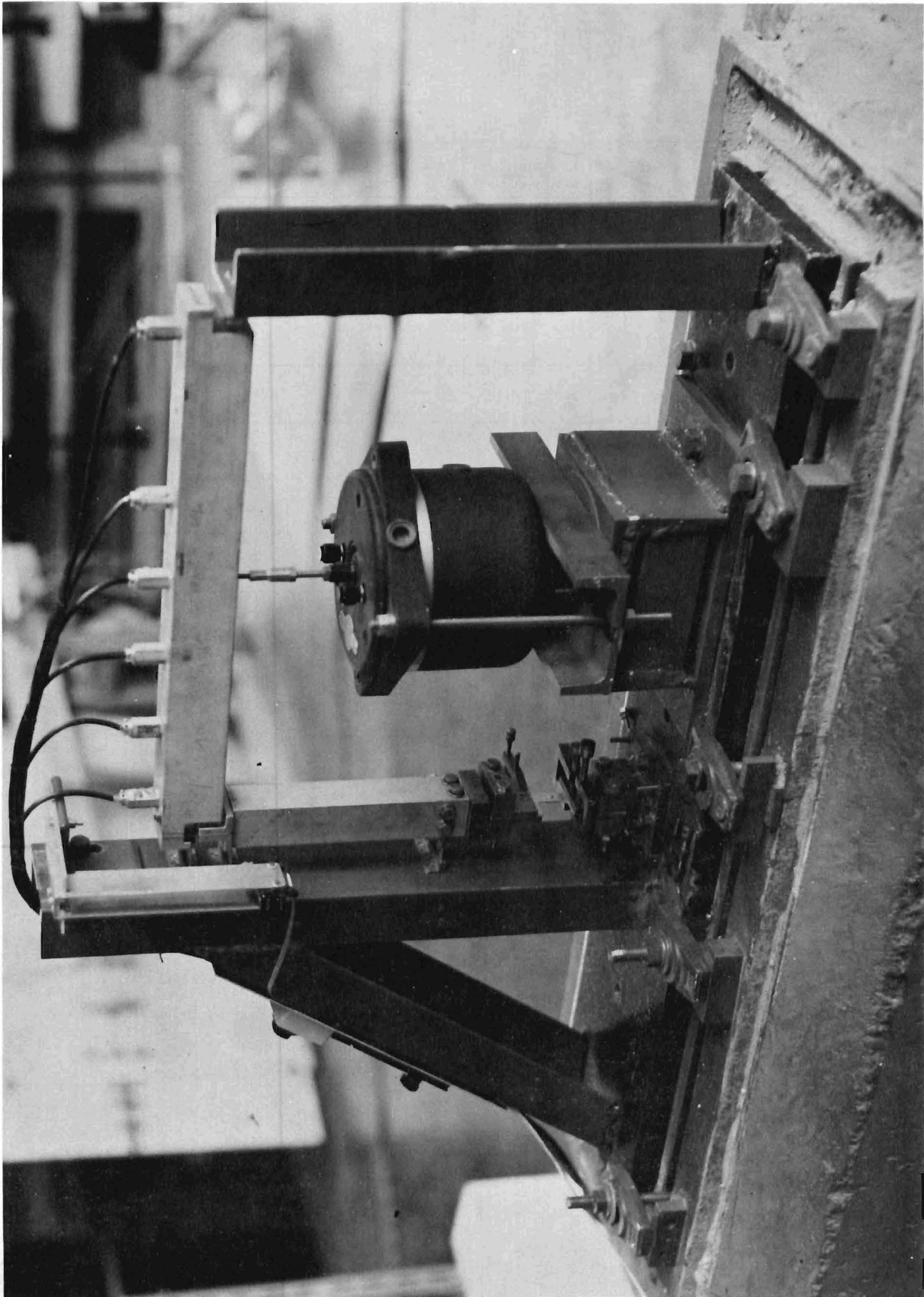


FIGURE 15. FATIGUE - RIG FOR TESTING RIVETED JOINTS.

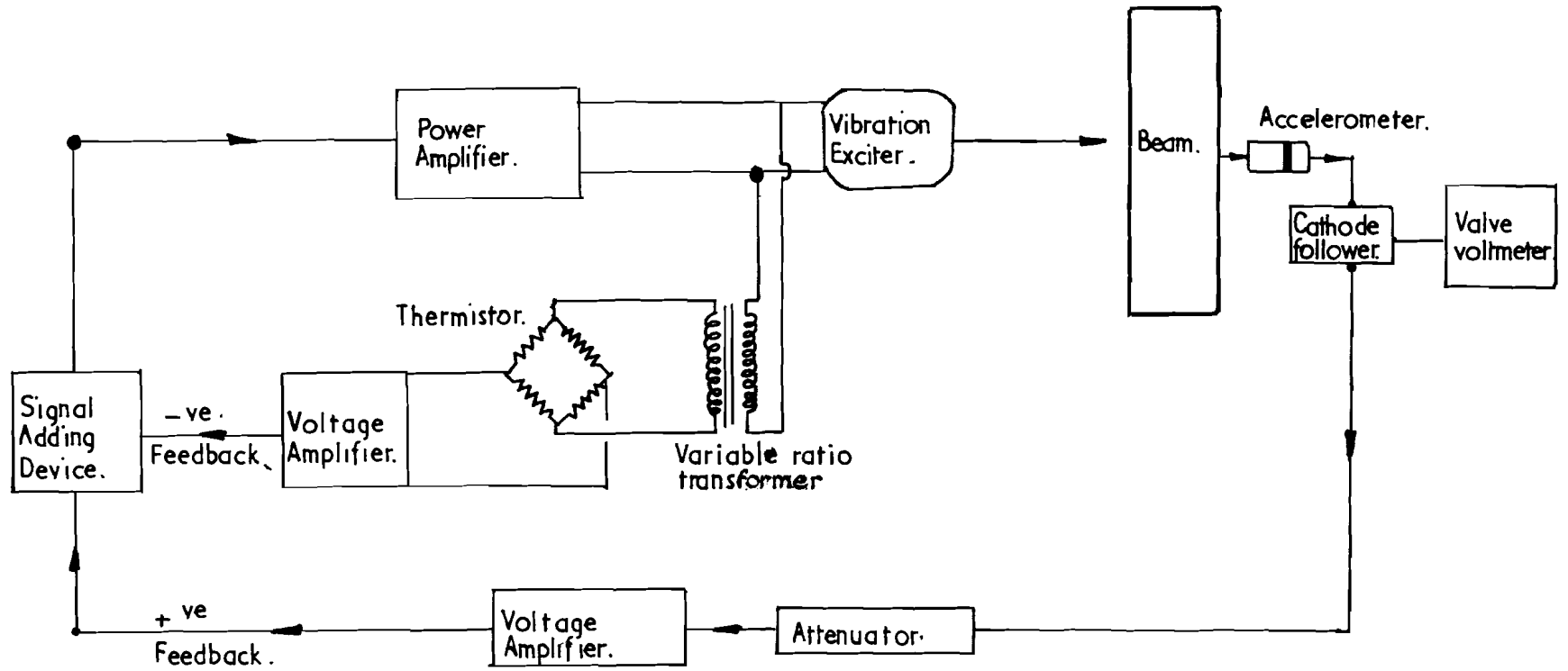


FIGURE 16 LINE DIAGRAM OF THE SELF EXCITED METHOD APPLIED TO THE FATIGUE RIG.

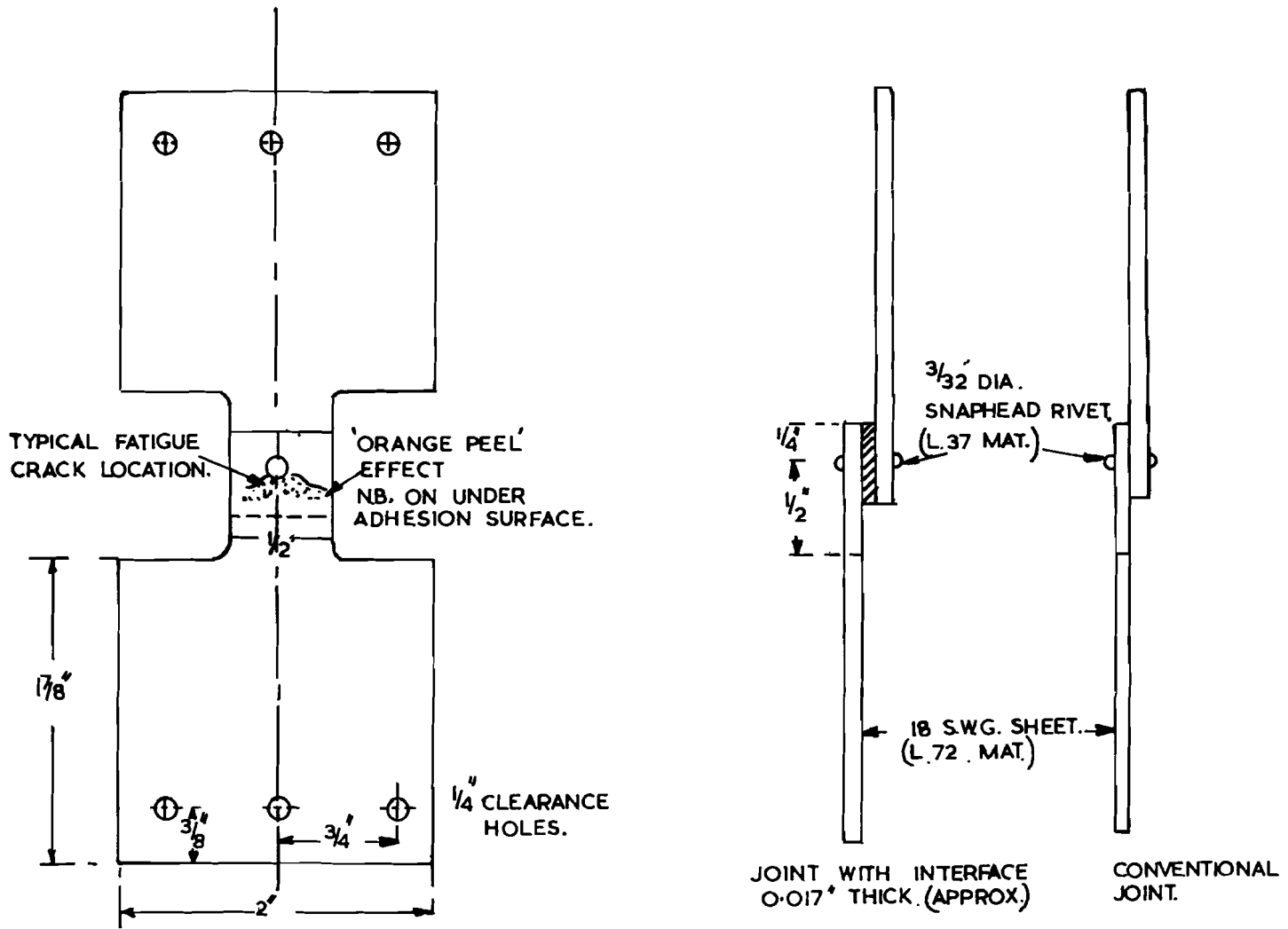


FIGURE 17. DETAILS OF THE FATIGUE TEST SPECIMENS.

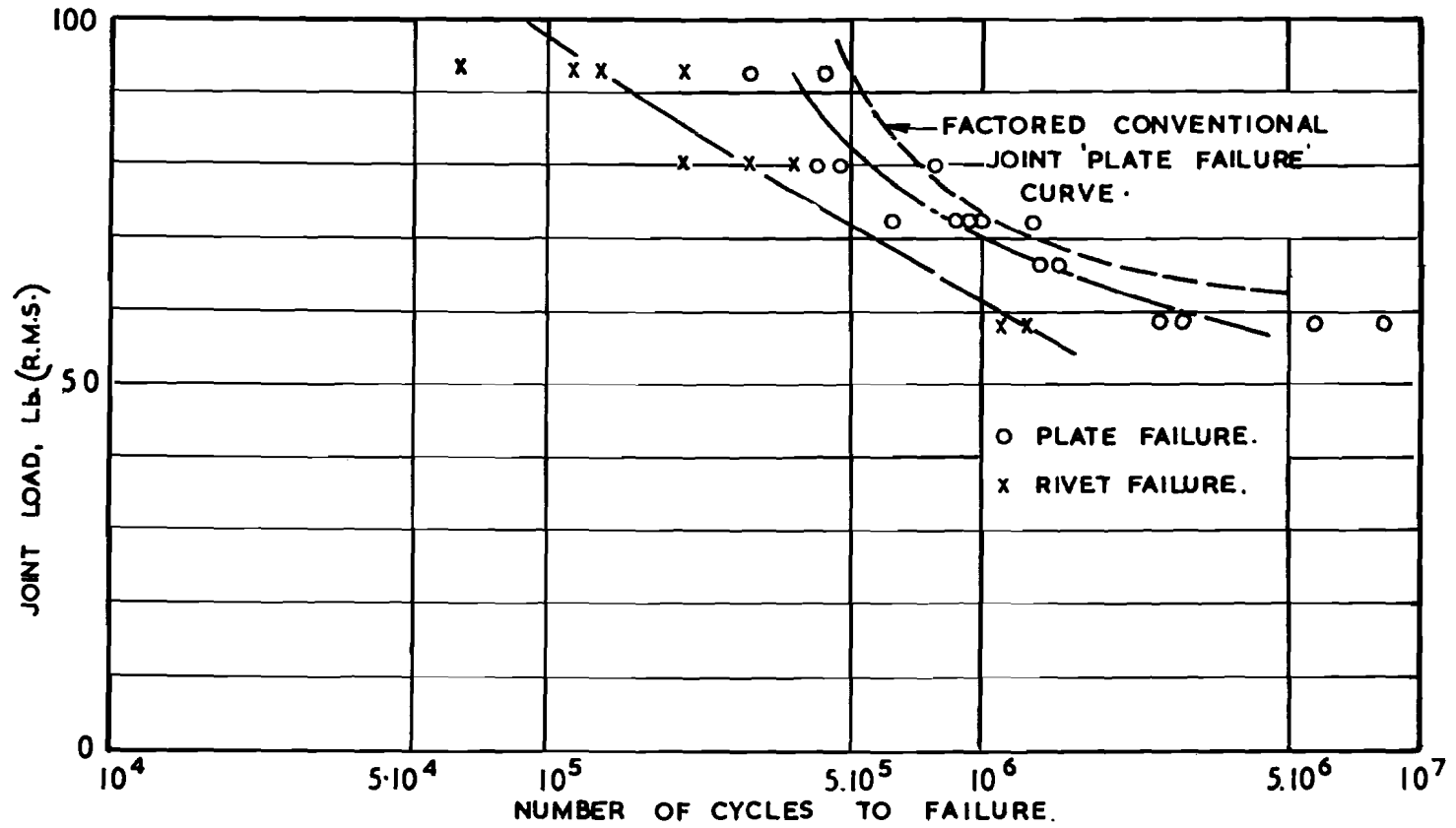


FIGURE 19. FATIGUE CURVES FOR A SINGLY RIVETED LAP JOINT WITH A VISCO-ELASTIC INTERFACE SUBJECTED TO SIMPLY HARMONIC LOADING.
JOINT TEMPERATURE $\approx 30^{\circ}\text{C}$

UNCLASSIFIED

Security Classification

DOCUMENT CONTROL DATA - R&D

(Security classification of title, body of abstract and indexing annotation must be entered when the overall report is classified)

1. ORIGINATING ACTIVITY (Corporate author) University of Southampton Southampton, England		2a. REPORT SECURITY CLASSIFICATION UNCLASSIFIED	
		2b. GROUP	
3. REPORT TITLE Interface Damping at Riveted Joints Part II: Damping and Fatigue Measurements			
4. DESCRIPTIVE NOTES (Type of report and inclusive dates)			
5. AUTHOR(S) (Last name, first name, initial) Eaton, D. C. G., Mead, Denys J.			
6. REPORT DATE August 1965		7a. TOTAL NO. OF PAGES 46	7b. NO. OF REFS 7
8a. CONTRACT OR GRANT NO. AF 61(052)-504		9a. ORIGINATOR'S REPORT NUMBER(S) ASD-TR-61-467, Part II	
b. PROJECT NO. 7351		9b. OTHER REPORT NO(S) (Any other numbers that may be assigned this report)	
c. Task No. 735106		d.	
10. AVAILABILITY/LIMITATION NOTICES Qualified requesters may obtain copies of this report from DDC.			
11. SUPPLEMENTARY NOTES		12. SPONSORING MILITARY ACTIVITY Metals and Ceramics Division Air Force Materials Laboratory Wright-Patterson AFB, Ohio 45433	
13. ABSTRACT <p>This report describes experiments to measure energy dissipated under harmonic loading at a riveted joint with a visco-elastic interfacial layer. Comparison is made with theoretical results from Part I, and reasonable agreement is found. Fatigue tests on damped joints show that the damping layer increases fatigue life for given applied load levels. Description is also given of apparatus developed for measuring complex shear modulus of layer material.</p>			

14. KEY WORDS	LINK A		LINK B		LINK C	
	ROLE	WT	ROLE	WT	ROLE	WT
Riveted Joints Interface Damping Damping and Fatigue Measurements Visco-elastic Complex Shear Modulus Apparatus						

INSTRUCTIONS

1. **ORIGINATING ACTIVITY:** Enter the name and address of the contractor, subcontractor, grantee, Department of Defense activity or other organization (*corporate author*) issuing the report.

2a. **REPORT SECURITY CLASSIFICATION:** Enter the overall security classification of the report. Indicate whether "Restricted Data" is included. Marking is to be in accordance with appropriate security regulations.

2b. **GROUP:** Automatic downgrading is specified in DoD Directive 5200.10 and Armed Forces Industrial Manual. Enter the group number. Also, when applicable, show that optional markings have been used for Group 3 and Group 4 as authorized.

3. **REPORT TITLE:** Enter the complete report title in all capital letters. Titles in all cases should be unclassified. If a meaningful title cannot be selected without classification, show title classification in all capitals in parenthesis immediately following the title.

4. **DESCRIPTIVE NOTES:** If appropriate, enter the type of report, e.g., interim, progress, summary, annual, or final. Give the inclusive dates when a specific reporting period is covered.

5. **AUTHOR(S):** Enter the name(s) of author(s) as shown on or in the report. Enter last name, first name, middle initial. If military, show rank and branch of service. The name of the principal author is an absolute minimum requirement.

6. **REPORT DATE:** Enter the date of the report as day, month, year; or month, year. If more than one date appears on the report, use date of publication.

7a. **TOTAL NUMBER OF PAGES:** The total page count should follow normal pagination procedures, i.e., enter the number of pages containing information.

7b. **NUMBER OF REFERENCES:** Enter the total number of references cited in the report.

8a. **CONTRACT OR GRANT NUMBER:** If appropriate, enter the applicable number of the contract or grant under which the report was written.

8b, 8c, & 8d. **PROJECT NUMBER:** Enter the appropriate military department identification, such as project number, subproject number, system numbers, task number, etc.

9a. **ORIGINATOR'S REPORT NUMBER(S):** Enter the official report number by which the document will be identified and controlled by the originating activity. This number must be unique to this report.

9b. **OTHER REPORT NUMBER(S):** If the report has been assigned any other report numbers (*either by the originator or by the sponsor*), also enter this number(s).

10. **AVAILABILITY/LIMITATION NOTICES:** Enter any limitations on further dissemination of the report, other than those

imposed by security classification, using standard statements such as:

- (1) "Qualified requesters may obtain copies of this report from DDC."
- (2) "Foreign announcement and dissemination of this report by DDC is not authorized."
- (3) "U. S. Government agencies may obtain copies of this report directly from DDC. Other qualified DDC users shall request through _____."
- (4) "U. S. military agencies may obtain copies of this report directly from DDC. Other qualified users shall request through _____."
- (5) "All distribution of this report is controlled. Qualified DDC users shall request through _____."

If the report has been furnished to the Office of Technical Services, Department of Commerce, for sale to the public, indicate this fact and enter the price, if known.

11. **SUPPLEMENTARY NOTES:** Use for additional explanatory notes.

12. **SPONSORING MILITARY ACTIVITY:** Enter the name of the departmental project office or laboratory sponsoring (*paying for*) the research and development. Include address.

13. **ABSTRACT:** Enter an abstract giving a brief and factual summary of the document indicative of the report, even though it may also appear elsewhere in the body of the technical report. If additional space is required, a continuation sheet shall be attached.

It is highly desirable that the abstract of classified reports be unclassified. Each paragraph of the abstract shall end with an indication of the military security classification of the information in the paragraph, represented as (TS), (S), (C), or (U).

There is no limitation on the length of the abstract. However, the suggested length is from 150 to 225 words.

14. **KEY WORDS:** Key words are technically meaningful terms or short phrases that characterize a report and may be used as index entries for cataloging the report. Key words must be selected so that no security classification is required. Identifiers, such as equipment model designation, trade name, military project code name, geographic location, may be used as key words but will be followed by an indication of technical context. The assignment of links, rules, and weights is optional.